Mining at scale with latent factor models for matrix completion

Fabio Petroni

Sapienza University of Rome, 2015

Mining at scale with latent factor models for matrix completion

Fabio Petroni

Ph.D. program in Engineering in Computer Science.
Department of Computer, Control, and Management
Engineering Antonio Ruberti
at Sapienza University of Rome

presented by
Fabio Petroni

Rome, 02/02/2016

Author:

Fabio Petroni

petroni@dis.uniroma1.it

`http://www.fabiopetroni.com`

Contents

Sommario

Predire quali relazioni è probabile che si verifichino tra oggetti del mondo reale è un compito fondamentale per diverse applicazioni. Ad esempio, i sistemi di raccomandazione automatici mirano a predire l'esistenza di relazioni sconosciute tra utenti e oggetti, e sfruttano tali informazioni per fornire suggerimenti personalizzati di oggetti potenzialmente d'interesse per uno specifico utente. Le tecniche di completamento di matrice mirano a risolvere questo compito, indentificando e sfruttando i fattori latenti che hanno innescato la creazione di relazioni note, al fine di dedurre quelle mancanti.

Questo problema, tuttavia, è reso difficile dalle dimensioni dei dataset odierni. Un modo per gestire tale mole di dati, in un ragionevole lasso di tempo, è quello di distribuire la procedura di completamento della matrice su un cluster di macchine. Tuttavia, gli approcci correnti mancano di efficienza e scalabilità, poiché, per esempio, non minimizzano la comunicazione o garantiscono un carico di lavoro equilibrato nel cluster.

Un ulteriore aspetto delle tecniche di completamento di matrice preso in esame è come migliorare la loro capacità predittiva. Questo può essere fatto, per esempio, considerando il contesto in cui le relazioni vengono catturate. Tuttavia, incorporare informazioni contestuali generiche all'interno di un algoritmo di completamento matrice è un compito difficile.

Nella prima parte di questa tesi vengono studiate soluzioni distribuite per il completamento della matrice e affrontate le questioni di cui sopra esaminando tecniche di suddivisione dell'input, basate su algoritmi di partizionamento di grafi. Nella seconda parte della tesi ci si concentra su tecniche di completamento di matrice consapevoli del contesto, fornendo soluzioni che possono essere applicate sia (i) quando le voci note nella matrice assumono più valori e sia (ii) quando assumono tutte lo stesso valore.

Abstract

Predicting which relationships are likely to occur between real-world objects is a key task for several applications. For instance, recommender systems aim at predicting the existence of unknown relationships between users and items, and exploit this information to provide personalized suggestions for items to be of use to a specific user. Matrix completion techniques aim at solving this task, identifying and leveraging the latent factors that triggered the the creation of known relationships to infer missing ones.

This problem, however, is made challenging by the size of today's datasets. One way to handle such large-scale data, in a reasonable amount of time, is to distribute the matrix completion procedure over a cluster of commodity machines. However, current approaches lack of efficiency and scalability, since, for instance, they do not minimize the communication or ensure a balance workload in the cluster.

A further aspect of matrix completion techniques we investigate is how to improve their prediction performance. This can be done, for instance, considering the context in which relationships have been captured. However, incorporating generic contextual information within a matrix completion algorithm is a challenging task.

In the first part of this thesis, we study distributed matrix completion solutions, and address the above issues by examining input slicing techniques based on graph partitioning algorithms. In the second part of the thesis, we focus on context-aware matrix completion techniques, providing solutions that can work both (i) when the revealed entries in the matrix have multiple values and (ii) all the same value.

CHAPTER 1

Introduction

The Web, they say, is leaving the era of search and entering one of discovery. What's the difference? Search is what you do when you're looking for something. Discovery is when something wonderful that you didn't know existed, or didn't know how to ask for, finds you.

Jeffrey M. O'Brien

Understanding the underlying causes that lead to the creation of relationships among objects is a crucial task to acquire a deeper knowledge of the world, and predict its evolution. While some relationships are relatively easy to capture and model, others, although present in the world, are by their nature difficult to represent, especially when their interpretation is hidden inside large amounts of data. The study of such relationships is essential in several scientific fields, ranging from biology to sociology, from physics to engineering, and its exploitation has led to several important advances in recent years. For instance, recent techniques for mineral exploration avoid deep holes to look for regions containing desirable materials, but just analyze samples near the surface [25]. By understanding the relationships among deeply buried mineral deposit and near-surface geochemistry it is possible to predict the location of the former without drilling, therefore minimizing the environmental impact. Similarly, the relationships between users in online social networks, which drastically changed the way people interact and communicate, are a rich source of information for computer and social sciences, but also for commercial purposes. For instance, by understanding the factors that led to two users to be friends, it is possible to predict and suggest other users with whom they might be interested to connect [77].

The current data production rate, however, poses additional challenges to the task of understanding and modeling such relationships. The last few years, in particular, have witnessed a huge growth in information production. Some corporations like IBM estimate that "2.5 quintillion bytes of data are created every day", amounting to 90% of the data in the world today having been created in the last two years [37]. For this reason, legacy approaches, based, for instance, on manual inspection, are being rapidly replaced by automatic data mining methods based on machine learning techniques, able to cope with data at such massive scale and to produce far better results. The term "data mining", indeed, derives from the metaphor of data as something that is very large, contains far too much information to be used, but can be mined to extract nuggets of valuable knowledge.

One successful approach to represent relationships, whose interpretation is hidden inside large scale dataset, is to model the objects as points in a d dimensional space. The dimensions of such space represent latent factors that originate the relationships. Each object is therefore modeled as a vector of real values, one for each considered latent factor. For instance, consider a person that likes the band Sex Pistols. A possible explanation for this "like" relationship is that the musical tastes of the person are geared toward punk music (factor one) and that he has a rebel character (factor two). Such explanation can be represented in a two-dimensional space, where dimensions correspond to the factor *punk music* and the factor *rebel character*. A two-dimensional vector is associated with both the user and the band, with and high value for the two factors, i.e., they lie close in the latent factor space. These factors are called "latent" because they are not directly observable in the data. Moreover, unlike this example, in real applications (1) it is often impossible to provide a clear interpretation for them and (2) the number of considered latent factors is much higher. By comparing the latent representations of different objects it is possible to derive the existence of unknown relationships among them. For instance, the system might predict that the above person also likes the band Ramones, since also this object has a vector representation with an high value for the two considered latent factors.

In this thesis we restrict our focus to binary relationships, that can be represented in the form of a matrix, where rows and columns represent objects, and entries report the interactions among them. For example, a matrix might represent friendship relationships between users in an online social network. In this case, rows and columns represent users and an entry equal to one indicates that the row user and the column user are friends. In many practical problems of interest, only a (usually really small) portion of entries in the data matrix are known. By leveraging the latent vector representation of objects is possible to complete the missing part of the matrix, adding new entries as coherent as possible with the observed data. For the sake of clarity, consider the following two scenarios, where such kind of matrix completion techniques have been successfully applied, as prototypical applications.

Collaborative Filtering in Recommender Systems. A recommender system collects the preferences that a set of users express on a set of items and, by exploiting this information, tries to provide personalized recommendations that fit the users' personal tastes. Several e-commerce leaders, like Amazon.com, Pandora and Netflix, have made recommender systems a crucial cornerstone of their data management infrastructure to boost their business offerings. In the last two decades, a consistent research effort has been devoted to the task of developing algorithms able to generate recommendations. The resulting research progress has established collaborative filtering (CF) techniques as the dominant framework for recommender systems [1, 121, 39, 103, 63]. Such methods look at the ratings of like-minded users to provide recommendations, with the idea that users who have expressed similar interests in the past will share common interests in the future. A large bunch of machine learning techniques have been exploited for collaborative filtering (see section 2.1.1). Among this multitude of algorithms, matrix completion techniques based on latent factor models have emerged as the best approach to collaborative filtering, due to their advantages with respect to both scalability and accuracy [123, 66, 73, 91]. The assumption behind such solutions is that only a few factors contribute to an individual's tastes or preferences. The data matrix in this case is composed with users as rows, item as columns and ratings as entries. By completing this matrix is possible to infer users' preferences for unrated items, and exploit these predictions to provide personalized recommendations.

Open Relation Extraction in Natural Language Processing. Relation extraction is concerned with predicting the existence of unknown relations (e.g., "was born in") among real word entities (e.g., persons, locations, organizations). These systems take in input a set of real word facts, expressed as relation-subject-object triples, and correlate them to estimate the likelihood of unobserved facts. For example, a relation extraction system may be fed with facts such as "is the singer of"("Thom Yorke", "Radiohead"), "is band member of"("Ringo Starr", "The Beatles"), etc. Several machine learning methods have been leveraged for relation extraction (see section 4.2.1); they can be broadly classified in closed and open approaches. Closed approaches [80, 86, 22] aim at predicting new facts for a predefined set of relations, usually taken from an existing knowledge base. Open relation extraction techniques [104, 30, 90], instead, aim at predicting new facts for a potentially unbounded set of relations, which come from various sources, such as natural language text and knowledge bases. One of the most successful techniques for open relation extraction is based on matrix completion [104, 90]. The corresponding data matrix is usually represented with relations as columns and subject-object pairs as rows; an entry equal to one means that a fact has been observed in input referring to the subject-object pair (in the row) and the relation (in the column). By completing the matrix it is possible to estimate the likelihood of each unobserved fact, associated with a missing entry in the data matrix, and to exploit this information to predict new facts. In the above example, for instance, the system might predict the fact "is band member of"("Thom Yorke", "Radiohead").

The above application scenarios have some peculiar characteristics and difficulties; for instance, one fundamental difference between the two is that in recommender systems users can usually provide both positive and negative feedback (e.g., on a zero-to-five scale) while a fact in natural language is either observed or not, i.e., there are only positive observations in input and no explicit negative evidence. The data matrix reflects these two scenarios, in that revealed entries have multiple values in the former case, all the same value in the latter case. This leads to two different ways to learn latent factor models able to complete the matrix.

One common characteristics of the above scenarios, and of general instances of the matrix completion problem, is that real applications may involve millions of objects and billions of entries in the matrix; for instance, Amazon.com offers thousands of products to more than 200M active customers, and, only in 2014, the number of purchases was estimated around 2B [120]. The amount of data available for such kind of systems is indeed a key factor for their effectiveness [49]. In order to cope with datasets at such massive scales, in a reasonable amount of time, parallel and distributed approaches are essential. Here we consider a general shared-nothing distributed architecture which allows asynchronous communication between computing nodes. The main challenges in this environment are concerned with the partitioning of the data matrix among the computing nodes; the goal is to distribute the data so that (1) each computing nodes operates on subsets of the data with minimum overlap with each other, in order to minimize the communication and (2) the workload is fairly balanced among nodes to maximize the efficiency. However, current solutions only partially solve the above challenges, in that they use simple or general purpose partitioning algorithms. For example, these techniques do not take into consideration common characteristics of the input data that can help in optimizing the data placement over the two aforementioned lines, as, for instance, the relationships power-law distribution, often visible in real data, i.e., most objects have relatively few relationships (e.g., niche movies rated by few) while a few have many (e.g., popular movies rated by many).

The overall performance of matrix completion solutions can be boosted not only feeding the system with more data [49], but also integrating contextual information in the model [90]. To have some insights on the economic value that a performance improvement in such systems can generate, consider that Netflix awarded a 10% boost in prediction accuracy for its recommendation system with $1M via the widely-publicized Netflix prize [12]. In many application domains, a context-agnostic approach to matrix completion may lose predictive power because potentially useful information from multiple contexts is aggregated. Even human understanding often requires the use of context. For example, the natural language relation "plays with"(x,y) is unspecific, possible meanings include play sports or play in a band. However, the comprehension can be facilitated if contextual information is available, for instance the topic of the document where the relation is extracted (e.g., sport, music, etc.).

The integration of generic contextual information within a matrix completion model is a relatively new line of research [2, 96, 97, 114]; some solutions have been proposed, mainly focused on collaborative filtering in recommender systems (see section 4.1). An open challenge in this domain is how to incorporate such contextual data when the system is fed only with positive feedback, that is when the revealed entries in the matrix have all the same value.

1.1 Contributions

This thesis deals with the aforementioned challenges, and provides scalable solutions for matrix completion, as well as efficient ways to integrate contextual information in the predictive model, even in those cases when the revealed entries in the matrix have all the same value (i.e., there is no negative evidence in input). Our contributions can be summarized as follows.

Distributed Matrix Completion.

We investigated distributed matrix completion solutions, able to perform the training procedure over a shared noting cluster of computing nodes, using as application scenario collaborative filtering in recommender systems. We review existing centralized, parallel (i.e., working on shared memory) and distributed approaches based on stochastic gradient descent, a popular technique used to learn the latent factor representations for the objects. We focus on asynchronous version of the stochastic gradient descend algorithm for large-scale matrix completion problems, and we propose a novel variant, namely GASGD, that leverages data partitioning schemes based on graph partitioning techniques and exploits specific characteristics of the input data to tackle the above challenges, that is to reduce the communication among computing nodes while maintaining the load balanced in the system. This approach looks at the input data as a graph where each vertex represents an object (i.e., either a row or a column) and each edge represents a relationship between the two vertices (i.e, an entry in the data matrix).

To partition the input data, we considered several state-of-the-art graph partitioning algorithms that consume the input data in a streaming fashion, thus imposing a negligible overhead to the overall execution time. However, existing graph partitioning solutions only partially exploit the skewed power-law degree distribution of real world dataset. To fill this gap, we propose *high degree (are) replicated first* (*HDRF*), a novel stream-based graph partitioning algorithm based on a greedy vertex-cut approach that effectively exploits skewed degree distributions by explicitly taking into account vertex degree in the placement decision. *HDRF* is characterized by the following desirable properties: (1) it outputs a partition with the smallest average replication factor among all competing solutions and (2) it provides close to optimal load balancing, even in those cases where classic greedy approaches typically fail. On the one hand, lowering the average replication factor is important to reduce network bandwidth cost, memory usage and replica synchronization overhead at computation time. A fair distribution of load in the partition, on the other hand, allows a more efficient usage of available computing resources. Both aspects, when put together, can positively impact the time needed to execute matrix completion and, in general, graph computation algorithms. Our experimental evaluation, conducted on popular real-word datasets, confirm that *HDRF* combines both these aspects; matrix completion algorithms run up to two times faster using *HDRF* as input partitioner with respect to state-of-the-art partitioning algorithms. We also report a theoretical analysis of the *HDRF* algorithm, and provide an upper bound for the replication factor.

Context-Aware Matrix Completion. We study context aware matrix completion solutions, able to incorporate generic contextual information within the predictive model. We review existing approaches, mainly proposed for collaborative filtering, that work with a matrix in which revealed entries have multiple values, that is when the system is fed with both positive and negative evidence. We proposed a novel algorithm to incorporate contextual data even in those cases in which the revealed entries in the matrix have all the same value, using as application scenario relation extraction, a popular natural language processing task. In particular, we propose CORE, a novel matrix completion model that leverages contextual information for open relation extraction. Our model integrates facts from various sources, such as natural language text and knowledge bases, as well as the context in which these facts have been observed. CORE employs a novel matrix completion model that extends existing context-aware solutions so as to work in those situations in which the system receive in input only positive feedback (i.e., observed facts). Our model is extensible, i.e., additional contextual information can be integrated when available. We conducted an experimental study on a real-world dataset; even with limited amount of contextual information used, our CORE model provided higher prediction performance than previous solutions.

CHAPTER 2

Matrix Completion

Essentially, all models are wrong, but some are useful.

George E. P. Box

Matrix completion is at its heart a technique to reconstruct a matrix for which only a small portion of entries are available. This task is related with general matrix factorization models, such as matrix reconstruction or non-negative matrix factorization [119]. In those cases, however, all entries in the matrix are available and need to be taken into consideration, and computing a low-rank model is relatively easy (e.g., through singular value decomposition [13, 108]). Matrix completion is, instead, impossible without additional assumptions, and, even with those, the problem is not only NP-hard, but all known algorithms require time doubly exponential in the dimension of the matrix [24, 21].

Approximated matrix completion methods have been proposed to reduce the computational cost of exact solutions, and, therefore, to be of practical interest. Such techniques are currently experiencing a growing interest in several fields of the data mining and machine learning community, driven by the enormous success they achieve in recommender systems, an application scenario that we will use as baseline for exposition.

2.1 Recommender Systems

For users today's world wide web it's the tyranny of choice. Consider that people on average read around ten megabytes (MB) worth of material a day; hear 400MB a day, and see one MB of information every second [38]. However, every 60 seconds 1500 blog entries are created, 98000 tweets are shared, and 600+ videos are uploaded to YouTube [84]. Studies have repeatedly shown that when people are confronted with too many choices their ability to make rational decisions declines [110]. Recommender systems aims at reducing such choices and make the life of the users easier.

Many of todays internet businesses strongly base their success in the ability to provide personalized user experiences. This trend, pioneered by e-commerce companies like Amazon [75], has spread to many different sectors. As of today, personalized user recommendations are commonly offered by internet radio services (e.g., Pandora Internet Radio), social networks (e.g., Facebook), media sharing platforms (e.g., YouTube) and movie rental services (e.g., Netflix). To estimate the economic value of such recommendations, consider that 2/3 of the movies watched on Netflix are recommended, recommendations generate 38% more clickthrough in Google news and 35% sales in Amazon came from recommendations [6]. In general, personalization techniques are considered the lifeblood of the social web [106].

A widely adopted approach to build recommendation engines is represented by collaborative filtering algorithms.

2.1.1 Collaborative Filtering

Collaborative filtering (CF) is a thriving subfield of machine learning, and several surveys expose the achievements in this fields [1, 121, 39, 103, 63]. The essence of CF lies in analyzing the known preferences of a group of users to make predictions of the unknown preferences for other users.

The first work on the field of CF was the Tapestry system [46], developed at Xerox PARC, that used a manual collaborative filtering system to filter mails, using textual queries, based on the opinion of other users, expressed with simple annotations (such as "useful survey" or "excellent"). Shortly after, the GroupLens system [102, 62] was developed, a pioneer application that gave users the opportunity to rate articles on a 1 to 5 scale and receive automatic suggestions. Quickly recommender systems and collaborative filtering became a hot topic in several research communities, ranging from machine learning to human–computer interaction, and a large number of algorithms started to be proposed. Moreover, in the same period, commercial deployments of recommender systems, pioneered

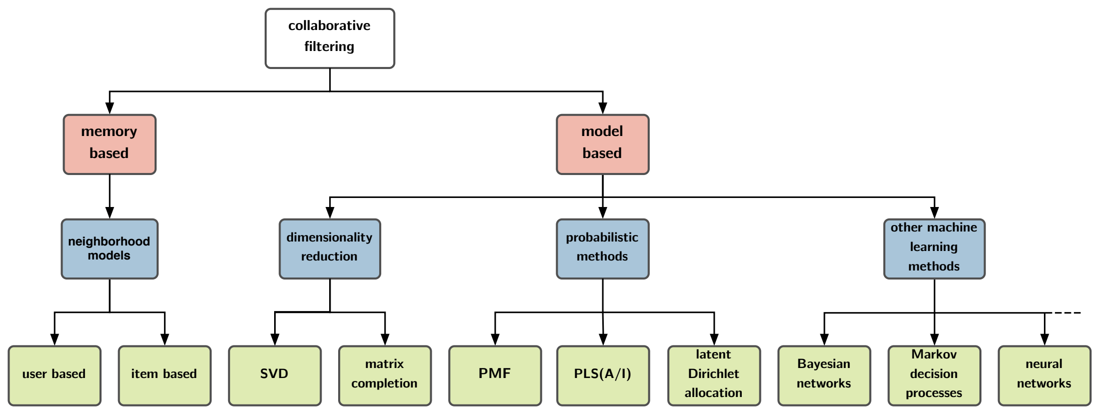

Figure 2.1: Taxonomy of collaborative filtering algorithms.

by companies such as Amazon.com, Yahoo! and Netflix, began to spread all over the world wide web. The effort of the community in this field experienced a significant boost in 2006, when Netflix launched a competition to improve their recommendation engine: the *Netflix prize* [12]. The objective of this open competition was to build a recommender algorithm that could improve the internal Netflix solution on a fixed dataset by 10%. The reward for the winner was US$1,000,000, an amount that demonstrate the importance of accurate recommendations for vendors. The Netflix prize triggered a feverish activity, both in academia and among hobbyists, that led to several advances and novel solutions.

It is possible to divide existing CF techniques in two main groups: *memory-based* and *model-based* [19, 1, 39] (see figure 2.1).

Memory-based algorithms operate on the entire database of ratings to compute similarities between users or items. Such similarities constitute the “memory” of the collaborative filtering system, and are successively exploited to produce recommendations. Similar users or items are identified using a similarity metric, such as the Pearson correlation coefficient [102] and the cosine similarity [10, 118], that analyzes and compares the rating vectors of either users or items. The basic idea is to generate predictions by looking at the ratings of the most similar users or items; for this reason such techniques are called *neighborhood models*.

Neighborhood models are categorized as *user based* or *item based*. User based methods compute a similarity score between each pair of users, and then estimate unknown ratings based on recorded ratings of similar users [51, 133, 113]. Item-oriented methods, instead, use the known ratings to compute similarities between items, and then provide recommendations by looking at similar items to those that an user has previously rated [109, 68, 33].

Memory-based methods are used in a lot of real-world systems because of their simple design and implementation. However, they impose several scalability limitations, since the computation of similarities between all pairs of users or items is expensive (i.e., quadratic time complexity with respect to the number of users or items), that makes their use impractical when dealing with large amounts of data.

<u>*Model-based*</u> approaches have been investigated to overcome the shortcomings of memory-based algorithms. They use the collection of ratings to estimate or learn a model and then apply this model to make rating predictions. A large amount of machine learning techniques have been used to build such model. In this multitude of algorithms, a noteworthy families of solutions are dimensionality reduction techniques.

The idea behind such solutions is to reduce the dimensionality of the rating space, in order to discover underlying structures that can be leveraged to predict missing ratings. Traditional collaborative filtering solutions, in fact, view the user-item ratings domain as a vector space, where a vector with an entry for each user is associated to each item, and vice-versa. These solutions aims at reducing the dimensionality of such vectors, and therefore of the domain space, to some fixed constant number d, so that both users and items can be represented as a d-dimensional vector. The underlying assumption is that the interaction between users and items (i.e., the ratings) can be modeled using just d factors. Such factors can be modeled explicitly, i.e., topics of interest, or can be considered latent in the ratings data. Latent representation of users and items can be extracted using singular value decomposition (SVD) [13, 108], a technique that decompose the rating matrix in three constituent matrices of smaller size, and exploit the factorization of them to predict missing ratings. However, SVD-based models can be applied only when the input matrix is complete. Since the rating matrix contains, by its nature, a large portion of missing values, some heuristics must be applied to pre-fill missing values; examples include, use the item's average rating or consider missing values as zeros.

Matrix completion techniques [64, 66, 123] avoid the necessity of pre-filling missing entries by reasoning only on the observed ratings. They can be seen as an estimate or an approximation of the SVD, computed using application specific optimization criteria. Such solutions are currently considered as the best single-model approach to collaborative filtering, as demonstrated, for instance, by several public competitions, such as the Netflix prize [12] and the KDD-Cup 2011 [35], and they will be extensively described in the rest of this thesis.

Another remarkable families of collaborative filtering solutions are probabilistic methods, that use statistical probability theory rather than linear algebra to predict missing ratings. Example of such methods include probabilistic matrix factorization (PMF) [81, 71], probabilistic latent semantic analysis/indexing (PLSA/I) [52, 56, 29] and latent Dirichlet allocation [14]. Other machine learning techniques for collaborative filtering include Markov decision processes [111], Bayesian networks [19, 137], and neural networks [105]. The main advantage of dimensionality reduction techniques over other existing solution is the availability of efficient parallel and distributed implementations, that make it possible to handle very large-scale instances of the problem, in a reasonable amount of time.

2.2 The Matrix Completion Problem

We consider a system constituted by $U = (u_1, \cdots, u_n)$ users and $X = (x_1, \cdots, x_m)$ items. Items represent a general abstraction that can be case by case instantiated as news, tweets, shopping items, movies, songs, etc. Users can either explicitly express their opinion by rating items with values from a predefined range (i.e., explicit feedback) or just provide an implicit indication of their taste (i.e., implicit feedback), for instance by clicking on a website. Without loss of generality, here we assume that ratings are represented with real numbers. By collecting user ratings it is possible to build a $n \times m$ rating matrix R that is usually a sparse matrix as each user rates a small subset of the available items. Denote by $O \subseteq \{1, ..., n\} \times$

Symbol	Description
R	Data matrix; rating matrix
n, m	Number of rows and columns of R
U	Users set; rows
X	Items set; columns
T	Training set; set of revealed entries in R
O	Set of indices identifying revealed entries
P, Q	Latent factor matrices
d	Dimensionality of the completion; rank of the factorization

Table 2.1: Notation for matrix completion algorithms in recommender systems.

$\{1, ..., m\}$ the set of indices identifying observed entries in R; $(i, j) \in O$ implies that user u_i rated (implicitly or explicitly) item x_j with vote r_{ij}. The training set is defined as $T = \{r_{ij} : (i, j) \in O\}$. The goal of a matrix completion algorithm is to predict missing entries $\widehat{r}_{ij}$ in R using ratings contained in the training set.

2.3 Latent Factor Models

Matrix completion approaches based on latent factors models represent the interactions between users and items using a fixed set of latent factors. Each user and item is represented through a vector of weights, one for each latent factor. In this way both users and items are placed in a *latent factor space*. The positioning in this space is driven by the preferences users expressed on items, in such a way that users with similar tastes are close together, as well as similar items. Moreover, users and items actually share the latent factor space; closer is an item to an user higher the estimated likelihood that such user actually likes the item.

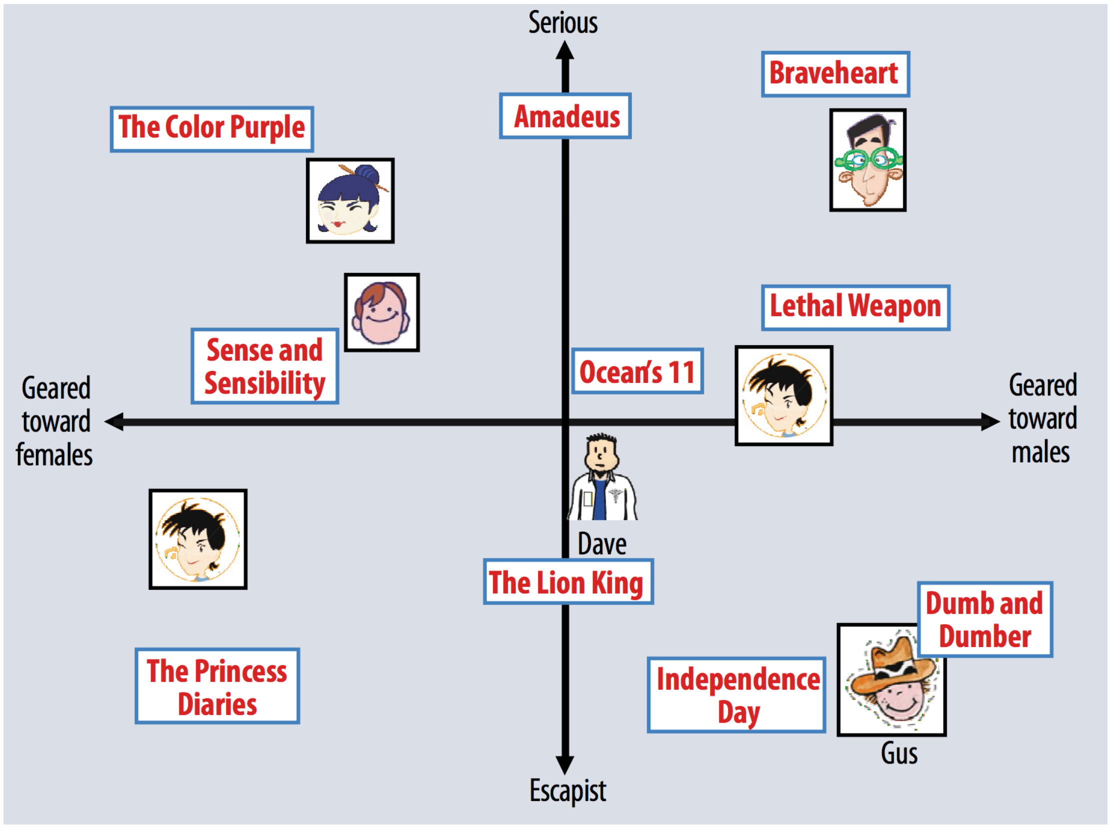

Figure 2.2: A simple example of factor space, with male versus female on the x-axis and serious versus escapist on the y-axis, taken from [66].

Figure 2.2 reports a classic example of two dimensions latent factor space, taken from [66], that shows where some well-knows movies and fictitious users might be positioned, using as factors the orientation towards male or female (x-axis) and towards serious or escapist (y-axis). For example, the model's prediction of the likelihood that user "Gus" likes movie "Dumb and Dumber" is very high, while is very low for the same user and the movie "The Color Purple". Note that some users (e.g., "Gus") and movies (e.g., "The Princess Diaries") are strongly polarized by these two dimensions, while other users (e.g., "Dave") and movies (e.g., "Ocean's") are neutral with

respect to them.
In real applications the number of latent factors is much higher (usually more than 100), and the dimension are often completely uninterpretable.
Denote by $d \ll min(n, m)$ the number of such latent factors, i.e., the dimensionality of the completion. Concretely, latent factors models for matrix completion aim at finding an $n \times d$ row-factor matrix P^* (*user vectors matrix*) and an $d \times m$ column-factor matrix Q^* (*item vectors matrix*) such that $R \approx P^* Q^*$. Denote with p_i, the i-th row of P – the d-dimensional latent factor vector associated with user u_i – and q_j, the j-th column of Q – the d-dimensional vector of item x_j.
The positioning of users and items in the latent factor space, as well as the likelihood estimations (e.g., rating prediction), hence the completion of the matrix, is performed computing the dot product between user and item vectors. The latent factor vectors are learned by minimizing (or maximizing) an application dependent objective function.

2.4 Optimization Criteria

In this section two classical optimization criteria for matrix completion are presented that, in recommender systems, are usually associated with the presence of explicit feedback (e.g., a rating from 1 to 5) or implicit feedback (e.g., purchase history) in the system. The main difference between these two scenarios is that in the former the matrix completion algorithm receives both negative and positive input, while in the latter only positive evidence exists.

2.4.1 Regularized Squared Loss

The regularized square loss [66, 123, 125, 136] is typically used when both positive and negative evidence is present in input, that is when the revealed entries in the matrix have multiple values. Classic examples are systems in which users are given the opportunity to express ratings on a zero to five stars scale (e.g., Netflix, Amazon.com, TripAdvisor, etc.).

The basic idea for the completion of the input matrix is that the new values (added to fill missing entries) must be as much coherent as possible with the existing data. If the portion of revealed entries is sufficiently large and close to uniformly distributed, one way to reconstruct the original matrix is adding entries in such a way to minimize the rank of the final matrix, that is seeking the simplest explanation that fits the observed data [21]. However, this approach is impractical since the corresponding optimization problem is NP-hard, and the time complexity of existing rank minimization algorithms is double exponential in the dimension of the matrix [21].

In practice, the most used optimization criterion is a relaxation of the rank minimization problems, that aims at minimizing the regularized square loss, defined as follows:

$$L(P,Q) = \sum_{(i,j)\in O} (r_{ij} - p_i q_j)^2 + \lambda(||P||_F^2 + ||Q||_F^2) \qquad (2.1)$$

where $|| \cdot ||_F$ is the Frobenius norm and $\lambda \geq 0$ is a model specific regularization parameter. The main advantage of this formulation is that it leads to a significant reduction in computation time: there exist algorithms to minimize $L(P,Q)$ that can efficiently handle very large instances of the matrix completion problem (see below). On the other hand, this optimization function is non-convex and thus it potentially has local minima that are not globally optimal.

The loss function can be more sophisticated than Equation 2.1, including user and item bias [123], time [65], implicit feedback [64], attributes and contextual data [100].

Finally note that Equation 2.1 is in *summation form* as it is expressed as a sum of *local losses* [125] L_{ij} for each element in R:

$$L_{ij}(P,Q) = (r_{ij} - p_i q_j)^2 + \lambda \sum_{k=1}^{r} (P_{ik}^2 + Q_{kj}^2) \qquad (2.2)$$

2.4.2 Bayesian Personalized Ranking

In real-world applications most feedback are implicit rather than explicit. Examples for such feedback include purchases in an online shop, views in a video portal or clicks on a website. Implicit feedback are much easier to collect, since users have not to express their taste explicitly. When only positive observations are present in input, the revealed entries in the matrix have all the same values. For ease of exposition, denote such entries with 1s in the matrix R. The previous optimization criterion is not effective when dealing with this situation, since the system simply complete the matrix with all 1s (in this way the final matrix has a minimum rank that is equal to one), and the resulting trained model is unable to predict anything (i.e., it predicts that everything is true or liked).

Actually, the underling matrix completion problem when dealing with revealed entries that have multiple values (e.g., explicit feedback) or all the same value (e.g., implicit feedback) is quite similar, the data is just different. In fact, even when the system detects only positive feedback, the original matrix is supposed to contain a mixture of both positive and negative data; however, the revealed entries are not uniformly distributed but all positive.

One of the most successful approaches to cope with this situation is based on the observation that the problem is actually related with ranking more than prediction. For instance, in recommender system the goal is to provide a personalized ranked list of items that the user might like the most. The Bayesian personalized ranking (BPR) [99, 89] is a well-known optimization criterion for this task, that has been successfully applied in several application scenarios, including tweet recommendation [23], link prediction [77], open relation extraction [104] and point of interest recommendation [67]. The BPR criterion adopts a pairwise approach, in that it aims at predicting whether item x_j is more likely to be bought than x_k from a specific user u (i.e. the user-specific order of two items), rather than the probability for pair (u, x_j) or (u, x_k). In particular, BPR assumes that user u prefers all the items for which a positive feedback exists (e.g., all the items that have been bought by user u) with respect to items without a feedback (e.g., not bought items). To formalize, denote with $D_T : U \times X \times X$ the training data, defined as:

$$D_T := \{(u_i, x_j, x_k) | u_i \in U \wedge x_j, x_k \in I, j \neq k \wedge r_{ij} = 1 \wedge r_{ik} = ?\}$$

The semantics of $(u_i, x_j, x_k) \in D_S$ is that user u_i is assumed to prefer item x_j over x_k. In practice, the BPR criterion aims at maximizing the following objective function:

$$\text{BPR-}\textsc{Opt}(P,Q) = \sum_{(u_i,x_j,x_k)\in D_T} \Big[\ln \sigma(p_i q_j - p_i q_k) \Big] + \lambda(||P||_F^2 + ||Q||_F^2) \tag{2.3}$$

where $\sigma(x) = \frac{1}{1+e^{-x}}$ denotes the logistic function and $\lambda \geq 0$ is a model specific regularization parameter.

A different application scenario for the BPR optimization criterion will be presented in chapter 4.

2.5 Stochastic Gradient Descent

The most popular technique to minimize or maximize the above objective functions is stochastic gradient descent (SGD). To be rigorous, this technique works in a "descendent" fashion when it is used to minimize a target objective function, such as $L(P,Q)$, while it works in an "ascendent" fashion when used to maximize a target objective function, such as BPR-$\textsc{Opt}(P,Q)$. In this latter case, the algorithm can be called stochastic gradient ascent.

It has been originally proposed by Simon Funk in a famous article on its blog [44] during the Netflix prize, and it radically changed the way in which the matrix completion problem is tackled. For instance, SGD was the approach chosen by the top three solutions of KDD-Cup 2011 [35]. SGD can be seen as a noisy version of gradient descent (GD). Starting from some initial point, GD works by iteratively updating current estimations of P and Q with values proportional to the negative of the gradient of the objective function.

For example, to minimize the regularized squared loss it iteratively computes:

$$P \leftarrow P - \eta \frac{\partial L(P,Q)}{\partial P}$$
$$Q \leftarrow Q - \eta \frac{\partial L(P,Q)}{\partial Q}$$

where η is the learning rate (a non-negative and finite parameter). GD is slow in practice, since the complete gradient of the objective function is expensive to compute. SGD, instead, combines implementation ease with a relatively fast running time. The term *stochastic* means that P and Q are updated by a small step for each given training point toward the average gradient descent. Intuitively, SGD performs many quick-and-dirty steps toward the minimum whereas GD perform a single expensive careful step. For example, to minimize the regularized squared loss, for each observed entry $(i,j) \in O$ the model variables are updated proportionally to the sub-gradient of the local loss (equation 2.2) over p_i and q_j, as follows:

$$p_i \leftarrow p_i - \eta \frac{\partial L_{ij}(P,Q)}{\partial p_i} = p_i + \eta(\varepsilon_{ij} \cdot q_j - \lambda p_i) \tag{2.4}$$
$$q_j \leftarrow q_j - \eta \frac{\partial L_{ij}(P,Q)}{\partial q_j} = q_j + \eta(\varepsilon_{ij} \cdot p_i - \lambda q_j) \tag{2.5}$$

where $\varepsilon_{ij} = r_{ij} - p_i q_j$ is the error between the real and predicted ratings for the (i,j) entry, and η is again the learning rate. Therefore, in each SGD step only the involved user and item vectors are updated; all other rows and columns remain unaffected. The algorithm proceeds performing several iterations through the available ratings until a convergence criterion is met. Several studies [83, 18] have shown that shuffling the training data before each *epoch*, that is a single iteration over the data, improve the convergence time for the algorithm.

The same technique can be applied to maximize the BPR objective function of equation 4.2. In this case the algorithm works by iteratively updating current estimations in the same direction of the stochastic gradient, in an ascendent fashion. A complete example of this will be exposed in chapter 4.

The SGD success stems also from the availability of efficient parallel and distributed implementations that make it possible to efficiently exploit modern multi-processor or cluster computing architectures to handle large scale matrix completion problems. Such solutions will be discussed in the next chapter.

2.6 Summary

The matrix completion problem arises in various applications in data mining including collaborative filtering in recommender systems, relational learning, and link prediction in social networks.

In this chapter, latent factor models for matrix completion have been presented, using as example application scenario collaborative filtering in recommender systems. Two standard optimization criteria have been exposed, to deal with both the presence of explicit and implicit feedback in the system, as well as a popular algorithm for parameter estimation, namely stochastic gradient descent.

CHAPTER 3

Distributed Matrix Completion

There are two possible outcomes: if the result confirms the hypothesis, then you've made a measurement. If the result is contrary to the hypothesis, then you've made a discovery.

Enrico Fermi

The SGD algorithm for matrix completion is, by its nature, inherently sequential; however, sequential implementations are usually considered poorly scalable as the time to convergence for large-scale problems may quickly grow to significant amounts. Parallel versions of SGD have been designed to overcome this problem by sharing the computation among multiple processing cores working on shared memory. The main challenge for parallel SGD solutions is that SGD updates might depend on each other. In particular, two threads may select training points referring to the same user (i.e., that lie in the same row) or to the same item (i.e., that lie in the same column). This brings both threads to concurrently update the same latent factor vector, associated with either the user or the item. This means that both threads might overwrite the work of the other, thus potentially affecting the final computation.

A natural approach to parallelize SGD across multiple threads is to divide the training points evenly among available t threads, such that each thread performs $|T|/t$ steps per epoch. To manage concurrent updates of shared variables and prevent overwriting each thread locks, before processing a training point $(i, j) \in O$, both row p_i and column q_j. However, lock-based approaches are known to adversely affect concurrency and, in the end, limit the scalability of the algorithm. HogWild [87] proposed a lock-free version of PSGD, where inconsistent updates are allowed. The idea in that, since the number of threads is usually much smaller than the number of rows or columns in the matrix, it is unlikely that two threads process the same vector. Even if this happen, it has been shown that these rare overwrites negligibly affect the final computation [87].

Other remarkable examples of shared memory SGD include Jellyfish [94] and two fast cache conscious approaches, namely CSGD [73] and FPSGD [136].

Beside these recent improvements, parallel SGD algorithms are hardly applicable to large-scale datasets, since the time-to-convergence may be too slow or, simply, the input data may not fit into the main memory of a single computer. Storing training data on disk is inconvenient because the two-dimensional nature of the rating matrix R will force non-sequential I/O making disk-based SGD approaches unpractical and poorly performant, although technically feasible. These problems recently motivated several research efforts toward distributed versions of SGD.

3.1 Distributed Stochastic Gradient Descend

This kind of algorithms [45, 125, 31, 3, 73, 91] are designed to work in a distributed shared-nothing environment, like, for instance, a cluster of commodity machines. This design allows to handle large scale instances of the matrix completion problem, which may exceed the main memory capacity of a single computing node. The key challenges faced by distributed SGD algorithms are: (1) minimize the communication while (2) balancing the workload, so that computing nodes are fed with roughly the same amount of data. An ideal solution should partition the input data in independent parts of equal size, such that each node operates on a disjoint part, no concurrent updates occur and the workload is balanced. In general, however, this is not achievable. To see this, depict the input data as a graph, where users and items are vertices and training points (e.g., ratings) edges. The ideal solution is achievable only when this graph is formed by several connected components (one for each computing node) with roughly the same number of edges. But this is in general not true as graphs representing real instances of the problem are usually connected.

In the sequel two families of distributed approaches will be discussed: stratified SGD [45, 125, 73] and asynchronous SGD [31, 3, 73, 91].

3.1.1 Stratified SGD

Stratified SGD (SSGD) [45] exploits the fact that some blocks of the rating matrix R are mutually independent (i.e., they share neither any row nor any column) so that the corresponding user and item vectors can be updated concurrently. For each epoch, several sequences of independent blocks of equal size (that constitute a *stratum*) are selected to cover the entire available data set. Then the algorithm proceeds by elaborating each stratum sequentially, assigning each block to a different computing node, until all the input data have been processed; at that point a new epoch starts. Figure 3.1

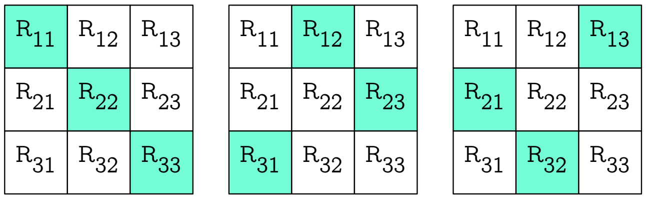
R_{11} R_{12} R_{13}
R_{21} R_{22} R_{23}
R_{31} R_{32} R_{33}

Figure 3.1: Example of stratum schedule used by SSGD in an epoch for a 3×3 blocking of R.

shows an example of a strata schedule during a single epoch, for a distributed setting with three computing nodes. The epoch starts with the first node processing block R_{11}, the second R_{22} and the third R_{33}. The blocks are independent so all vectors updates can be done concurrently. When computing nodes finish, they communicate all the updated column vectors to the next node. For instance, the first node send its updated column vectors (the first third of the entire columns set) to the third node, because it will need them to process block R_{31}. Then, a new stratum is processed, and so on for all strata.

The SSGD algorithm forms the basis of DSGD-MR [125], a MapReduce extension of SSGD, and DSGD++ [73], an efficient version of SSGD where a thread in each computing node is reserved to continuously communicate vectors' updates.

However, these solutions only partially solve the above challenges. On the one side, the workload balance is not guaranteed, since different blocks might contain a different number of entries; this is partially mitigated by shuffling rows and columns of R before creating the blocks, but the behavior with respect to load balancing remains only probabilistic. On the other side, the communication is quite intensive because, in each epoch, all item vectors (or user vectors) are exchanged between computing nodes.

3.1.2 Asynchronous SGD

An alternative approach to distribute SGD is represented by asynchronous SGD (ASGD) [31, 3, 73, 91]. ASGD distributes the matrix R among the set of available computing nodes, so that each of them only owns a slice of the input data. A problem with such approach is that, in general, the input partitioner is forced to assign ratings expressed by a single user (resp. received by a single item) to different computing nodes, in order to maintain the load in the system balanced. Thereby, user and item vectors must be concurrently updated, during the SGD procedure, by multiple nodes. A common solution is to replicate vectors on all the nodes that will work on them, forcing synchronization among the replicas via message exchange.

Given that each node has a local view of the vectors it works on, the algorithm needs to keep vector replicas on different nodes from diverging. This is achieved in two possible ways: either by maintaining replicas always in synch by leveraging a locking scheme (*synchronous* approach), or by letting nodes concurrently update their local copies and then periodically resynchronizing diverging vectors (*asynchronous* approach). Synchronous distributed SGD algorithms all employ some form of locking to maintain vector copies synchronized. This approach is however inefficient, because computing nodes spend most of their time in retrieving and delivering vector updates in the network, or waiting for lock to be released. The strictly sequential computation order imposed by this locking approach on shared vector updates negatively impacts the performance of such solutions.

Differently from synchronous algorithms, in ASGD computing nodes are allowed to concurrently work on shared user/item vectors, that can therefore deviate inconsistently during the computation. The system defines for each vector a unique *master copy* and several *working copies*. In the following we will refer to the node that store the master copy of a vector as *master node*. Each computing node updates only the local working copy of p_i and q_j[1] while processing training point $(i, j) \in O$. The synchronization between working copies and master is performed periodically according to the *Bulk Synchronous Processing* (BSP) model [47].

Initially all the vector copies are synchronized with their corresponding masters. At the beginning of an epoch, each computing node

[1]Also the vector master node updates a local working copy.

shuffles the subset data that it owns. Then, each epoch consists of:

1. a computation phase, where each node updates the local working copy of user and item vectors using data it owns;
2. a global message transmission phase, where each node sends all the vector working copies that have been updated in the previous phase to the corresponding masters;
3. a barrier synchronization, where each master node collects all the vector working copies, compute the new vector values, and sends back the result.

New vector values, computed in phase three, are usually obtained by averaging the working copies [76]. In [127] an exhaustive theoretical study of the convergence of ASGD is presented.

The algorithm can also work in a completely asynchronous fashion [125, 73], avoiding the BSP model. With this setting nodes can communicate continuously, they do not wait that every other node has completed its pass (the concept of epoch vanishes), and masters continuously average received working copies and send back updated values.

The problem is, again, how to balance the load among the computing nodes and minimize the communication. A common approach to input data partition is to grid the rating matrix R in $|C|$ blocks and then assign each block to a different computing node [125]. This partitioning approach clearly cannot guarantee a balanced number of ratings for each block, thus can possibly cause strong load imbalance among computing nodes. The problem can be mitigated by applying some random permutations of columns and rows. While this approach improves the load balancing aspect, it still lead to non negligible skews in the rating distributions (see section 3.3 for an empirical evaluation of this aspect). Furthermore, a second problem of the grid partitioning approach is that the communication cost between the computing nodes is not considered as a factor to be minimized. Matrix blocking, in fact, is performed without considering the relationships connecting users with items in R. As a consequence, the number of replicas for each user/item vector can possibly grow to the number of available computing nodes.

Graph-based Asynchronous Stochastic Gradient Descend

Graph-based asynchronous SGD (GASGD) [91] is a variant of ASGD that represents the input data as a bipartite graph, where users and items are associated with vertices and ratings with edges. This new data format doesn't change the ASGD algorithm, but allows (1) to provide input slicing solution based on graph partitioning algorithms and (2) to implement the SGD algorithm on top of distributed graph-computing (DGC) frameworks (such as GraphLab [69] or Pregel [74]). We consider a part in the partitioning for each computing node.

The above challenges can be easily adapted to the graph based representation. One goal is to fairly balance the edges (i.e., the training points) among parts. A second goal is to replicate each vertex in the minimum number of parts (ideally in a single part), so that only few computing nodes own a working copy of the corresponding latent factor vector, and the communication among them is minimized.

Note that graphs representing real instances of the matrix completion problem usually have a skewed power-law degree distribution, that is most users (resp. items) express (resp. receive) relatively few ratings while a few express (resp. receive) many. Exploiting this characteristic might be beneficial for a input partitioning algorithm, and, as a result, for the execution time of the matrix completion procedure.

3.2 Input Partitioner

The way the input dataset is partitioned has a large impact on the performance of GASGD and, in general, to whichever computation on the graph. A naive partitioning strategy may end up replicating a large fraction of the input elements on several parts, severely hampering performance by inducing a large replica synchronization overhead during the computation phase. Furthermore, the partitioning phase should produce evenly balanced parts (i.e., parts with similar sizes) to avoid possible load skews in a cluster of machines over which the data is partitioned.

Several recent approaches have looked at this problem. Here we focus our attention on *stream-based* graph partitioning algorithms, i.e., algorithms that partition incoming elements one at a time on the basis of only the current element properties and on previous assignments to parts (no global knowledge on the input graph). Furthermore, these algorithms are usually *one-pass*, i.e., they refrain from changing the assignment of a data element to a part once this has been done. Such algorithms are the ideal candidates in settings where input data size and constraints on available resources restrict the type of solutions that can be employed, as, for instance, those situations in which the graph exceeds the main memory capacity or the partitioning time should be minimized.

Other characteristics of input data also play an important role in partitioning. It has been shown that vertex-cut algorithms are the best approach to deal with input graphs characterized by power-law degree distributions [5, 47]. This previous work also clearly outlined the important role high-degree nodes play from a partitioning quality standpoint. Nevertheless, few algorithms take this aspect into account [131, 93]. Understandably, this is a challenging problem to solve for stream-based approaches due to their *one-pass* nature.

3.2.1 Problem Definition

The problem of optimally partitioning a graph to minimize vertex-cuts while maintaining load balance is a fundamental problem in parallel and distributed applications as input placement significantly affects the efficiency of algorithm execution [128]. An edge-cut partitioning scheme results in parts that are vertex disjoint while a vertex-cut approach results in parts that are edge disjoint. Both variants are known to be NP-Hard [60, 42, 7] but have different characteristics and difficulties [60]; for instance, one fundamental difference between the two is that a vertex can be cut in multiple ways and span several parts while an edge can only connect two parts.

One characteristic observed in real-world graphs from social networks or the Web is their skewed power-law degree distribution: most vertices have relatively few connections while a few vertices have many. It has been shown that vertex-cut techniques perform better than edge-cut ones on such graphs (i.e., create less storage and network overhead) [47]. For this reason modern graph parallel processing frameworks, like GraphLab [70], adopt a vertex-cut approach to partition the input data over a cluster of computing nodes. Here we focus on streaming vertex-cut partitioning schemes able to efficiently handle graphs with skewed power-law degree distribution.

Notation. Consider a graph $G = (V, E)$, where V is the set of vertices and E the set of edges. We define a partition of edges $S = (s_1, .., s_w)$ to be a family of pairwise disjoint sets of edges (i.e., $s_i, s_j \subseteq E$, $s_i \cap s_j = \emptyset$ for every $i \neq j$). Let $A(v) \subseteq S$ be the set of parts each vertex $v \in V$ is replicated. The size $|s|$ of each part $s \in S$ is defined as its edge cardinality, because computation steps are usually associated with edges. Since we consider G having a power-law degree distribution, the probability that a vertex has degree d is $P(d) \propto d^{-\alpha}$, where α is a positive constant that controls the "skewness" of the degree distribution, i.e., the smaller the value of α, the more skewed the distribution.

Balanced k-way vertex-cut problem. Given a graph G and a number of parts $|S|$, the problem consists in defining a partition of edges such that (i) the average number of vertex replicas (i.e., the number

Symbol	Description
G	Graph
V	Vertices
E	Edges
S	Partition
$A(v)$	Set of parts each vertex $v \in V$ is replicated

Table 3.1: Notation for graph partitioning algorithms.

of parts each vertex is associated to as a consequence of edge partitioning) is minimized and (ii) the maximum partition load (i.e., the number of edges associated to the biggest part) is within a given bound from the theoretical optimum (i.e., $|E|/|S|$) [7]. More formally, the balanced $|S|$-way vertex-cut partitioning problem aims at solving the following optimization problem:

$$\min \frac{1}{|V|} \sum_{v \in V} |A(v)| \quad s.t. \quad \max_{s \in S} |s| < \sigma \frac{|E|}{|S|} \tag{3.1}$$

where $\sigma \geq 1$ is a small constant that defines the system tolerance to load imbalance. The objective function (equation (3.1)) is called *replication factor* (RF), which is the average number of replicas per vertex.

Streaming setting. Without loss of generality, here we assume that the input data is a list of edges, each identified by the two connecting vertices and characterized by some application-related data. We consider algorithms that consume this list in a streaming fashion, requiring only a single pass. This is a common choice for several reasons: (i) it handles situations in which the input data is large enough that fitting it completely in the main memory of a single

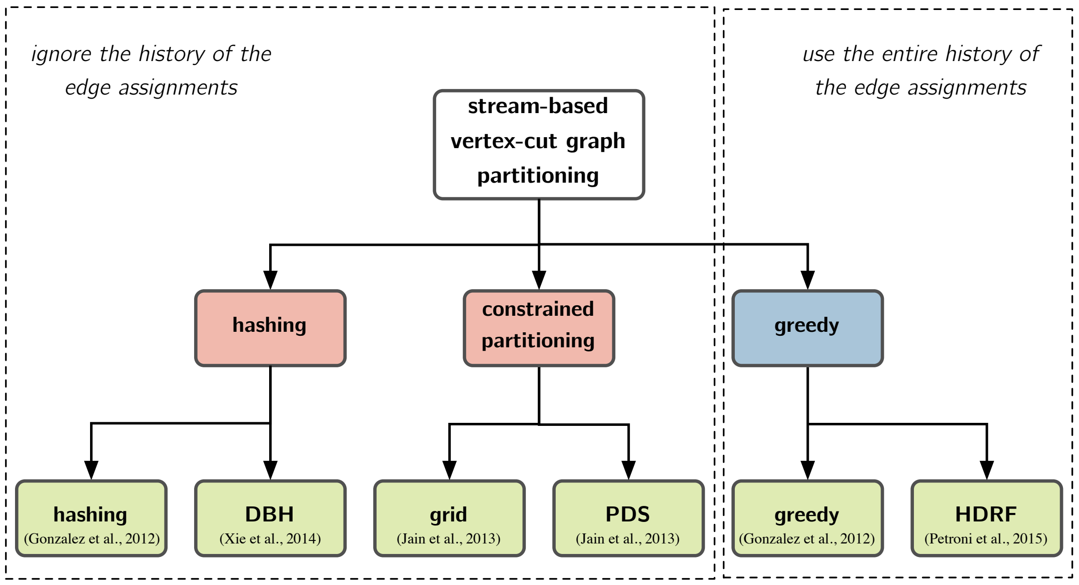
ignore the history of the edge assignments
use the entire history of the edge assignments
stream-based vertex-cut graph partitioning
hashing
constrained partitioning
greedy
hashing (Gonzalez et al., 2012)
DBH (Xie et al., 2014)
grid (Jain et al., 2013)
PDS (Jain et al., 2013)
greedy (Gonzalez et al., 2012)
HDRF (Petroni et al., 2015)

Figure 3.2: Taxonomy of stream-based vertex-cut graph partitioning algorithms.

computing node is impractical; (ii) it can efficiently process dynamic graphs; (iii) it imposes the minimum overhead in time and (iv) it's scalable, providing for straightforward parallel and distributed implementations. A limitation of this approach is that the assignment decision taken on an input element (i.e., an edge) can be based only on previously analyzed data and cannot be later changed.

3.2.2 Streaming Algorithms

Balanced graph partitioning is a well known NP-hard problem with a wide range of applications in different domains. It is possible to divide existing streaming vertex-cut partitioning techniques in two main families: "hashing and constrained partitioning algorithms" and "greedy partitioning algorithms" (see figure 3.2).

Hashing and constrained partitioning algorithms. All of these algorithms ignore the history of the edge assignments and rely on the presence of a predefined hash function $h : \mathbb{N} \to \mathbb{N}$. The input of the hash function h can be either the unique identifier of a vertex or of an edge. All these algorithms can be applied in a streaming setting and achieve good load balance if h guarantees uniformity. Four well-known existing heuristics to solve the partitioning problem belong to this family: *hashing*, *DBH*, *grid* and *PDS*. The simplest solution is given by the *hashing* technique that pseudo-randomly assigns each edge to a part: for each input edge $e \in E$, $A(e) = h(e) \bmod |S|$ is the identifier of the target part. This heuristic results in a large number of vertex-cuts in general and performs poorly on power-law graphs [47]. A recent paper describes the *Degree-Based Hashing* (*DBH*) algorithm [131], a variation of the *hashing* heuristic that explicitly considers the degree of the vertices for the placement decision. *DBH* leverages some of the same intuitions as *HDRF* by cutting vertices with higher degrees to obtain better performance. Concretely, when processing edge $e \in E$ connecting vertices $v_i, v_j \in V$ with degrees d_i and d_j, *DBH* defines the hash function $h(e)$ as follows:

$$h(e) = \begin{cases} h(v_i), & \text{if } d_i < d_j \\ h(v_j), & \text{otherwise} \end{cases}$$

Then, it operates as the *hashing* algorithm.

The *grid* and *PDS* techniques belong to the *constrained partitioning* family of algorithms [54]. The general idea of these solutions is to allow each vertex $v \in V$ to be replicated only in a small subset of parts $Z(v) \subset S$ that is called the *constrained set* of v. The constrained set must guarantee some properties; in particular, for each $v_i, v_j \in V$: (i) $Z(v_i) \cap Z(v_j) \neq \emptyset$; (ii) $Z(v_i) \nsubseteq Z(v_j)$ and $Z(v_j) \nsubseteq Z(v_i)$; (iii) $|Z(v_i)| = |Z(v_j)|$. It is easy to observe that this approach naturally imposes an upper bound on the replication factor. To position a new edge e connecting vertices v_i and v_j, it picks a part from the intersection between $Z(v_i)$ and $Z(v_j)$ either randomly or by choosing the least loaded one. Different solutions differ in the composition of the vertex constrained sets. The *grid* solution arranges parts in a $a \times b$ matrix such that $|S| = ab$. It maps each vertex v to a matrix cell using a hash function h, then $Z(v)$ is the set of all the parts in the corresponding row and column. It this way each constrained sets pair has at least two parts in their intersection. *PDS* generates constrained sets using *Perfect Difference Sets* [48]. This guarantees that each pair of constrained sets has exactly one part in their intersection. *PDS* can be applied only if $|S| = a^2+a+1$, where a is a prime number.

Greedy partitioning algorithms. This family of methods uses the entire history of the edge assignments to make the next decision. The standard *greedy* approach [47] breaks the randomness of the hashing and constrained solutions by maintaining some global status information. In particular, the system stores the set of parts $A(v)$ to which each already observed vertex v has been assigned and the current size of each part. Concretely, when processing edge $e \in E$ connecting vertices $v_i, v_j \in V$, the *greedy* technique follows this simple set of rules:

Case 1: If neither v_i nor v_j have been assigned to a part, then e is placed in the part with the smallest size in S.

Case 2: If only one of the two vertices has been already assigned (without loss of generality assume that v_i is the assigned vertex) then e is placed in the part with the smallest size in $A(v_i)$.

Case 3: If $A(v_i) \cap A(v_j) \neq \emptyset$, then edge e is placed in the part with the smallest size in $A(v_i) \cap A(v_j)$.

Case 4: If $A(v_i) \neq \emptyset$, $A(v_j) \neq \emptyset$ and $A(v_i) \cap A(v_j) = \emptyset$, then e is placed in the part with the smallest size in $A(v_i) \cup A(v_j)$ and a new vertex replica is created accordingly.

Symmetry is broken with random choices. An equivalent formulation consists of computing a score $C^{\text{greedy}}(v_i, v_j, s)$ for all parts $s \in S$, and then assigning e to the part s^* that maximizes C^{greedy}. The score consists of two elements: (i) a replication term $C^{\text{greedy}}_{\text{REP}}(v_i, v_j, s)$ and (ii) a balance term $C^{\text{greedy}}_{\text{BAL}}(s)$. It is defined as follows:

$$C^{\text{greedy}}(v_i, v_j, s) = C^{\text{greedy}}_{\text{REP}}(v_i, v_j, s) + C^{\text{greedy}}_{\text{BAL}}(s) \tag{3.2}$$

$$C^{\text{greedy}}_{\text{REP}}(v_i, v_j, s) = f(v_i, s) + f(v_j, s) \tag{3.3}$$

$$f(v, s) = \begin{cases} 1, & \text{if } s \in A(v) \\ 0, & \text{otherwise} \end{cases}$$

$$C^{\text{greedy}}_{\text{BAL}}(s) = \frac{\text{maxsize} - |s|}{\epsilon + \text{maxsize} - \text{minsize}} \tag{3.4}$$

where *maxsize* is the maximum part size, *minsize* is the minimum part size, and ϵ is a small constant value.

3.2.3 The HDRF Algorithm

High degree are replicated first (*HDRF*) [92] is a greedy algorithm tailored for skewed power-law graphs. In the context of robustness to network failure, Cohen et al. [26, 27] and Callaway et al [20] have analytically shown that if only a few high-degree vertices (hubs) are removed from a power-law graph then it is turned into a set of isolated clusters. Moreover, in power-law graphs, the clustering coefficient distribution decreases with increase in the vertex degree [34]. This implies that low-degree vertices often belong to very dense sub-graphs and those sub-graphs are connected to each other through high-degree vertices.

HDRF leverages these properties by focusing on the locality of low-degree vertices. In particular, it tries to place each strongly connected component with low-degree vertices into a single part by cutting high-degree vertices and replicating them on a large number of parts. As the number of high-degree vertices in power-law graphs is very low, encouraging replication for only these vertices leads to an overall reduction of the replication factor.

Concretely, when *HDRF* creates a replica, it does so for the vertex with the highest degree. However, obtaining degrees of vertices for a graph that is consumed in a streaming fashion is not trivial. To avoid the overhead of a pre-processing step (where the input graph should be fully scanned to calculate the vertex exact degrees), a table with partial degrees of the vertices can be maintained that is continuously updated while input is analyzed. As each new edge is considered in the input, the degree values for the corresponding vertices are updated in the table. The partial degree values collected at runtime are usually a good indicator for the actual degree of a vertex since it is more likely that an observed edge belongs to a high-degree vertex rather than to a low-degree one.[2]

More formally, when processing edge $e \in E$ connecting vertices v_i and v_j, the *HDRF* algorithm retrieves their partial degrees and increments them by one. Let $\delta(v_i)$ be the partial degree of v_i and $\delta(v_j)$ be the partial degree of v_j. The degree values are then normalized such that they sum up to one:

$$\theta(v_i) = \frac{\delta(v_i)}{\delta(v_i) + \delta(v_j)} = 1 - \theta(v_j) \tag{3.5}$$

As for the greedy heuristic, the *HDRF* algorithm computes a score $C^{\text{HDRF}}(v_i, v_j, s)$ for all parts $s \in S$, and then assigns e to the part s^* that maximizes C^{HDRF}. The score for each part $s \in S$ is defined as follows:

$$C^{\text{HDRF}}(v_i, v_j, s) = C^{\text{HDRF}}_{\text{REP}}(v_i, v_j, s) + C^{\text{HDRF}}_{\text{BAL}}(s) \tag{3.6}$$

$$C^{\text{HDRF}}_{\text{REP}}(v_i, v_j, s) = g(v_i, s) + g(v_j, s) \tag{3.7}$$

$$g(v, s) = \begin{cases} 1 + (1 - \theta(v)), & \text{if } s \in A(v) \\ 0, & \text{otherwise} \end{cases}$$

$$C^{\text{HDRF}}_{\text{BAL}}(s) = \mu \cdot C^{\text{greedy}}_{\text{BAL}}(s) = \mu \cdot \frac{\text{maxsize} - |s|}{\epsilon + \text{maxsize} - \text{minsize}} \tag{3.8}$$

The μ parameter allows control of the extent of part size imbalance in the score computation. We introduced this parameter because the standard *greedy* heuristic may result in an highly imbalanced

[2]While evaluating HDRF performance, we noticed no significant improvements in the algorithm performance when using exact degrees instead of their approximate values.

partition, especially when the input is ordered somehow. To see this problem note that $C_{\text{BAL}}^{\text{greedy}}(s)$ (equation 3.4) is always smaller than one, while $C_{\text{REP}}^{\text{greedy}}$ and $C_{\text{REP}}^{\text{HDRF}}$ are either zero or greater than one. For this reason, the balance term C_{BAL} in the *greedy* algorithm or when $0 < \mu \leq 1$ is used only to choose among parts that exhibit the same value for the replication term C_{REP}, thereby breaking symmetry.

However, this may not be enough to ensure load balance. For instance, if the stream of edges is ordered according to some visit order on the graph (e.g., breadth first search or depth first search), when processing edge $e \in E$ connecting vertices v_i and v_j there is always a single part s^* with $C_{\text{REP}}^{\text{greedy}}(v_i, v_j, s^*) \geq 1$ (resp. $C_{\text{REP}}^{\text{HDRF}}(v_i, v_j, s^*) > 1$) and all the other parts $s \in S$ s.t. $s \neq s^*$ have $C_{\text{REP}}^{\text{greedy}}(v_i, v_j, s) = 0$ (resp. $C_{\text{REP}}^{\text{HDRF}}(v_i, v_j, s) = 0$). In this case, the balance term is useless as there is no symmetry to break, and the heuristic ends up placing all edges in a single part s^*. This problem can be solved by setting a value for $\mu > 1$. In our evaluation (section 3.3), we empirically studied the trend of the replication factor and the load balance by varying μ (figure 3.12). Moreover, note that when $\mu \to \infty$ the algorithm resembles a random heuristic, where past observations are ignored and it only matters to have parts with equal size. The following summarizes the behavior of the *HDRF* algorithm with respect to the μ parameter:

$$\begin{cases} \mu = 0, & \text{agnostic of the load balance} \\ 0 < \mu \leq 1, & \text{balance used to break the symmetry} \\ \mu > 1, & \text{balance importance proportional to } \mu \\ \mu \to \infty, & \text{random edge assignment} \end{cases}$$

When $\mu = 1$ the *HDRF* algorithm can be represented by a set of simple rules, exactly as in *greedy*, with the exception of *Case 4* that is modified as follows:

Case 4 If $A(v_i) \neq \emptyset$, $A(v_j) \neq \emptyset$ and $A(v_i) \cap A(v_j) = \emptyset$, then

- if $\delta(v_i) < \delta(v_j)$, e is assigned to the part with the smallest size $s^* \in A(v_i)$ and a new replica of v_j is created in s^*;
- if $\delta(v_j) < \delta(v_i)$, e is assigned to the part with the smallest size $s^* \in A(v_j)$ and a new replica of v_i is created in s^*.

HDRF can be run as a single process or in parallel instances to speed up the partitioning phase. As with *greedy*, *HDRF* also needs some state to be shared among parallel instances during partitioning. In particular, we noticed that sharing the values of $A(v)$, $\forall v \in V$ is sufficient to let *HDRF* perform at its best.

3.2.4 Theoretical Analysis

In this section we characterize the *HDRF* algorithm behavior from a theoretical perspective, focussing on the vertex replication factor. In particular we are interested in an average-case analysis of *HDRF*. A worst-case analysis would provide poor performance, as expected for any similar greedy algorithm, while failing to capture the typical behavior of *HDRF* in real cases. In the rest of this section we assume $\mu = 1$ for the sake of simplicity.

Cohen et al. [27] considered the problem of a scale-free network (characterized as a power-law graph) attacked by an adversary able to remove a fraction c of vertices with the largest degrees. In particular they characterized the approximate maximum degree $\tilde{M}$ observable in the graph's largest component after the attack. If $|V| \gg 1/c$ this value can be approximated by the following equation:

$$\tilde{M} = mc^{1/(1-\alpha)} \tag{3.9}$$

where m is the (global) minimum vertex degree and α is the parameter characterizing the initial vertex degree distribution.

Let us now consider the algorithm *aHDRF* as an approximation of *HDRF*: *aHDRF* performs exactly as *HDRF*, but for the fact that we assume it knows the exact degree of each input vertex (and not the observed degree as for *HDRF*).

Theorem 1. *Algorithm aHDRF achieves a replication factor, when applied to partition a graph with $|V|$ vertices on $|S|$ parts, that can be bounded by:*

$$RF \leq \tau|S| + \frac{1}{|V|(1-\tau)} \sum_{i=0}^{|V|(1-\tau)-1} \left[1 + m \left(\tau + \frac{i}{|V|} \right)^{\frac{1}{1-\alpha}} \right]$$

$$\tau = \left(\frac{|S|-1}{m} \right)^{1-\alpha}$$

Proof. The replication factor bound is the sum of two distinct pieces. The first piece considers the fraction τ of vertices with the largest degrees in the graph, referred to as *hubs*. The worst case for hubs is to be replicated in all the parts, with a corresponding replication factor of $\tau|S|$. τ represents the fraction of vertices that must be removed from the graph such that the maximum vertex degree in the remaining graph is $|S|-1$; this value is obtainable through equation (3.9) by imposing $\tilde{M} = |S|-1$.

The second piece of the equation considers the contribution to the replication factor from non-hub vertices, i.e., all vertices whose degree is expected to be smaller than $|S|-1$ after the τ vertices with the largest degrees have been removed from the graph (together with their edges). When *aHDRF* processes an edge connecting a hub vertex with a non-hub vertex, it always favors the replication of the hub vertex (that has a larger degree) and replicates the non-hub vertex only if executes *Case 1* or *Case 2*, that is only if it is the first time it observes that vertex. Since the degree of non-hub vertices, ignoring the connections with hub vertices, is bounded by $m\tau^{1/(1-\alpha)}$, and since the connections with hub vertices can produce at most one replica, the worst case replication factor for non-hub vertices is bounded by:

$$\frac{1}{|V|(1-\tau)}\left(1+m\tau^{\frac{1}{1-\alpha}}\right)$$

This bound can be further improved by considering what happens to the graph once the non-hub vertex v_0 with the largest degree is removed. The previous bound is valid for v_0. However, the removal of v_0 from the graph will change the degree distribution, thus also reducing the bound for the next non-hub vertex with the largest degree. Using this consideration, it is possible to iteratively bound the degree of each non-hub vertex v_i with $m(\tau + i/|V|)^{1/(1-\alpha)}$ where $0 \leq i \leq |V|(1-\tau)-1$. Hence, the total worst case replication factor for non-hub vertices, is bounded by:

$$\frac{1}{|V|(1-\tau)}\sum_{i=0}^{|V|(1-\tau)-1}\left[1+m\left(\tau+\frac{i}{|V|}\right)^{\frac{1}{1-\alpha}}\right]$$

□

If edges arrive in random order, *aHDRF* gives an approximation of *HDRF*. In this case, the observed values for vertex degrees are a good estimate for the actual degrees. We can conclude that, assuming random order arrival for edges, *HDRF* is expected to achieve a replication factor, when applied to partition a graph with $|V|$ vertices on $|S|$ parts, of at most RF of Theorem 1.

For example, consider a graph with $\alpha = 2.2$, $|S| = 128$, $m = 1$ and 1M vertices. The average-case upper bound for the replication factor of *HDRF* is ≈ 5.12 while the actual result it achieves is ≈ 1.37. The bounds for *DBH* and *hashing* [47, 131] with this configuration are respectively ≈ 5.54 and ≈ 5.88, while the actual results they achieve are ≈ 1.89 and ≈ 2.52.

The upper bound given by Theorem 1 cannot be extended to other algorithms (e.g., *greedy*). Informally, *HDRF breaks* network at hubs by replicating a small fraction of vertices with large degrees. In contrast, *greedy* and other algorithms are agnostic to the degree of vertices when replicating them. Intuitively, these algorithms try to break network by removing *random* vertices. Unfortunately, power-law graphs are resilient against removing random vertices (see [26] for details). This implies that, in order to fragment a scale-free network, a very large number of random vertices should be removed. In other words, *greedy* and other algorithms tend to replicate a large number of vertices in different parts. This intuition is verified in our experiments (see section 3.3).

3.3 Evaluation

This section presents experimental results for the *HDRF* partitioning algorithm, with a particular focus to the benefits it generates on the GASGD algorithm when used as input partitioner. The evaluation was performed on real-world graphs by running the proposed algorithm both in a stand-alone partitioner (useful for scaling up to large parts number) and running an implementation of *HDRF* integrated into GraphLab.[3] The evaluation also reports experiments on synthetic graphs generated randomly with increasingly skewed distributions to study the extent to which *HDRF* performance is sensitive to workload characteristics.

3.3.1 Experimental Settings and Test Datasets

Evaluation Metrics. We evaluate the performance of *HDRF* by measuring the following metrics:

Replication factor: is the average number of replicas per vertex. This metric is a good measure of the synchronization overhead and should be minimized.

Load relative standard deviation: is the relative standard deviation of the number of edges hosted in target parts. An optimal partitioning strategy should have a value for this metric close to 0.

Max part size: is the number of either vertices or edges hosted in the largest part. We consider this metric with respect to both vertices and edges as each conveys different information. Edges are the main input for the computation phase, thus more edges in a part mean more computation for the computing node hosting it; conversely, the number of vertices in the system, and, therefore, in the largest part, also depends on the number of replicas generated by the partitioning algorithm.

[3]HDRF has been integrated into the official GraphLab PowerGraph source code `https://github.com/dato-code/PowerGraph`. The stand-alone software package for one-pass vertex-cut balanced graph partitioning is available at `https://github.com/fabiopetroni/VGP`.

Dataset	$\|V\|$	$\|E\|$
Tencent Weibo	1.4M	140M
Netflix	497.9K	100.4M
MovieLens 10M	80.6K	10M
twitter-2010	41.7M	1.47B
uk-2002	18.5M	298M
arabic-2005	22.7M	640M

Table 3.2: Statistics for real-world graphs.

Execution time: is the number of seconds needed by the DGC framework to perform the indicated computation on the whole input graph. Better partitioning, by reducing the number of replicas, is expected to reduce the synchronization overhead at runtime and thus reduce the execution time as well.

Datasets. In our evaluation, we used as datasets both synthetic power-law graphs and real-word graphs. The former were used to study how *HDRF* performance vary when the degree distribution skewness of the input graph gradually increases. In particular, each synthetic graph was generated with 1M vertices, minimum degree of 5 and edges using a power law distribution with α ranging from 1.8 to 4.0. Therefore, the number of edges in the graphs ranges from $\sim$ 60M ($\alpha = 1.8$) to $\sim$ 3M ($\alpha = 4$). Graphs were generated with *gengraph* [129].

We also tested the performance of *HDRF* on real-world graphs. We selected three bipartite preference graphs from the recommender systems community: *Tencent Weibo* from KDD-Cup 2012 [88], *Netflix* from the Netflix Prize [12] and *MovieLens 10M* made available by

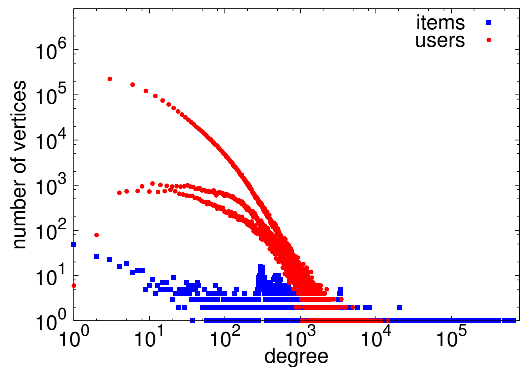

(a) Tencent Weibo

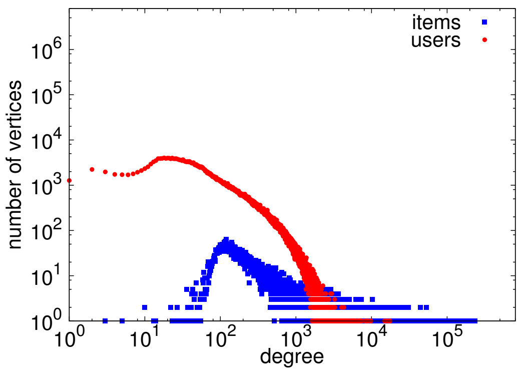

(b) Netflix

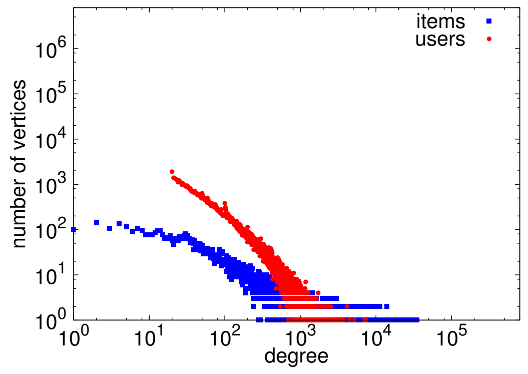

(c) MovieLens 10M

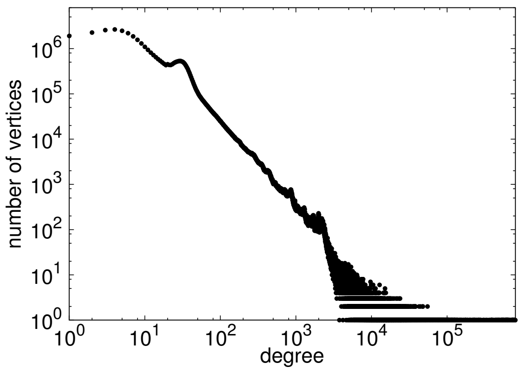

(d) twitter-2010

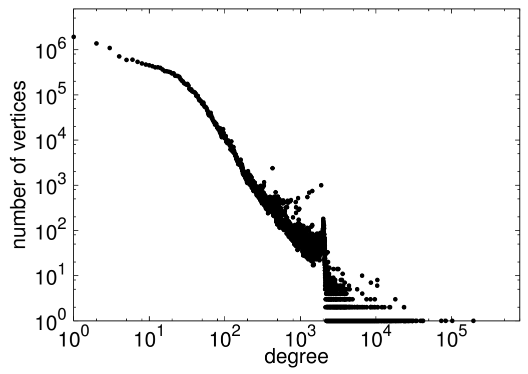

(e) uk-2002

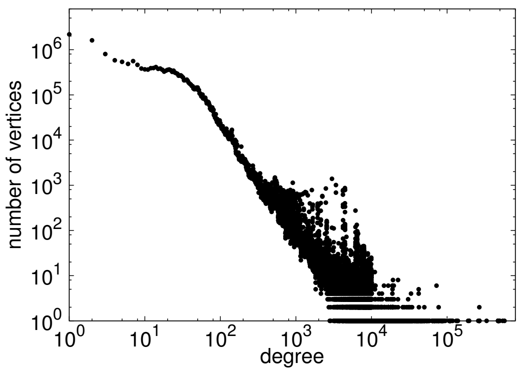

(f) arabic-2005

Figure 3.3: Degree distribution for real-world graph (log-log scale). For bipartite preference graphs the degree distribution for both users and items is reported.

the GroupLens research lab.[4] These were used to test in which ex-

[4]`http://grouplens.org/`

tent the GASGD algorithm benefits from the *HDRF* partitioning scheme, both in execution time and convergence speed. We also selected another 3 graphs from LAW (Laboratory for Web Algorithmics) [16, 15]: *twitter-2010*, *uk-2002* and *arabic-2005*. The latter were used to test the behavior of HDRF in a more general environment.

Table 3.2 reports some statistics for these 6 datasets, while figure 3.3 shows their degree distribution.

System Setup. We implemented a stand-alone version of a graph partitioner that captures the behavior of a DGC framework during the graph loading and partitioning phase. Within our partitioner, we implemented the five different algorithms described so far: *hashing*, *DBH*, *grid*, *PDS*, *greedy* and *HDRF*. Furthermore, we compared *HDRF* against two offline methods: *Ginger* [93], an hybrid solution that tries to combine both edge-cut and vertex-cut approaches together, and METIS [59], a well-known edge-cut partitioning algorithm. To compute the replication factor delivered by METIS, we used the same strategy of [47]: every edge-cut forces the two spanned parts in maintaining a replica of both vertices and a copy of the edge data. Experiments were run on an *Intel Xeon* 8-core machine with 32*GB* of memory running the GNU/Linux 64-bit operating system.

To run realistic tests needed to measure execution time, we implemented and integrated *HDRF* into GraphLab v2.2. In each test, we loaded and partitioned the input graph using *HDRF* or one of the comparison algorithms. Experiments with GraphLab where conducted both: (1) on an Amazon EC2 cluster, consisting of 31[5] m3.large[6] Linux instances in the US West (Oregon) region, and (2) on a cluster consisting of 8 machines with dual 16-core *Intel Xeon* CPUs and $128GB$ of memory each, where we experimented with 32, 64 and 128 parts by running multiple instances on a single machine.

We also evaluated the convergence of GASGD with respect to different input partitioner strategy, using a simulator.[7] As parameters, we used $d = 100$ latent factors, $\lambda = 0.05$ for all variables, a constant learning rate of $\eta = 0.005$, and ran 100 epochs.

Data input order. Since the input dataset is consumed as a stream of edges, the input order can affect the performance of the partitioning algorithm. We considered three different stream orders as in [128]: *random*, where edges arrive according to a random permutation; *BFS*, where the edge order is generated by selecting a vertex uniformly at random and performing a breadth first search visit starting from that vertex; *DFS*, that works as *BFS* except for the visit algorithm that is depth-first search. All reported results are based on a *random* input order unless otherwise mentioned in the text.

3.3.2 Performance Evaluation

The experimental results reported in this section are organized as follows: we first report on experiments that show the benefits that

[5]This number of parts fits constraints for *PDS*.

[6]2 vCPU and 7.5 Memory (GB)

[7]The source code is available at `https://github.com/fabiopetroni/GASGD`.

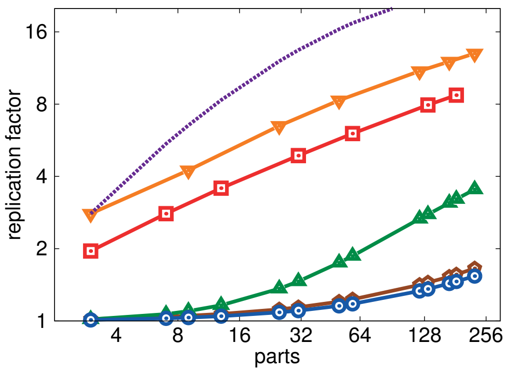

(a) Tencent Weibo

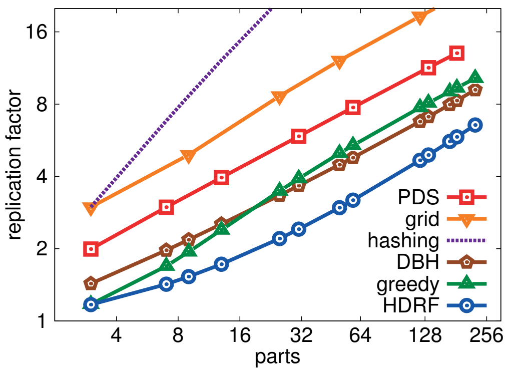

(b) Netflix

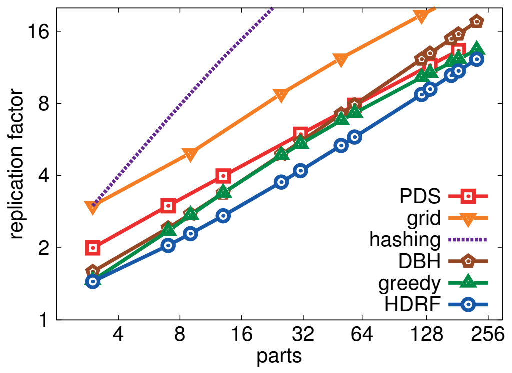

(c) MovieLens 10M

Figure 3.4: Replication factor varying the number of target parts (log-log scale).

HDRF brings to GASGD and, in general, the ability of *HDRF* to deliver the best overall performance in terms of execution time with the smallest overhead (replication factor) and close to optimal load balance when executed on real-world graphs. We then study how *HDRF* performance is affected by changes in the characteristics of the input dataset and changes in the target number of parts. Finally, the last set of results analyze the sensitivity of *HDRF* to input stream ordering.

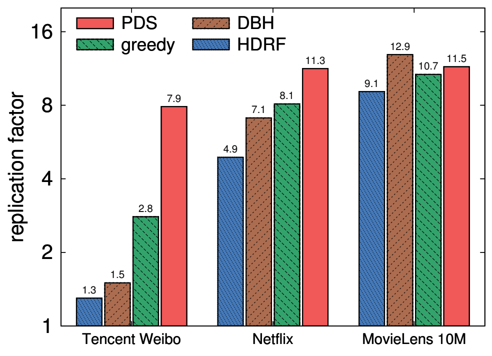

(a) Streaming algorithms

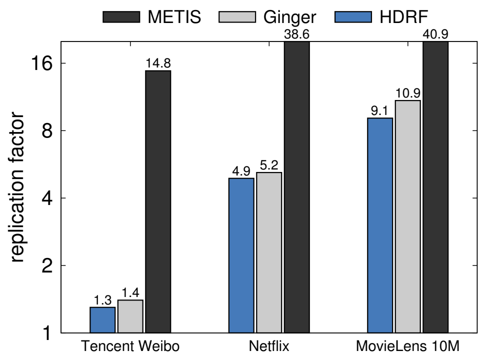

(b) Offline algorithms

Figure 3.5: Replication factor (log scale) with $|S| = 133$. *HDRF* is compared against both streaming and offline solutions.

GASGD Runtime

We first measured *HDRF* performance against other streaming partitioning algorithms on our set of real-world bipartite preference graphs. These experiments were run by partitioning the input graphs on a set of target parts in the range $[3, 256]$ with our stand-alone partitioner. Figure 3.4 reports the replication factor that the considered partitioning algorithms achieve on the different input graphs.[8] Moreover, figure 3.5a provides a snapshot of the evaluation, by setting the number of target parts to 133, a number compliant with PDS constraints. It can be observed that *HDRF* is the algorithm that provides the smallest replication factor for all the considered datasets.

In particular, for the Weibo dataset it is possible to observe how *HDRF* and *DBH* are the best performers as they both exploit vertex degrees. In all the other datasets *HDRF* is always the best per-

[8]Due to specific constraints imposed by the *PDS* and *grid* algorithms on the total number of parts, their data points are not aligned with those of the other algorithms.

former, albeit with larger absolute RF values. Summarizing, on the considered datasets *HDRF* achieves on average a replication factor about 40% smaller than DBH, more than 50% smaller than *greedy*, almost 3× smaller than *PDS*, more than 4× smaller than *grid* and almost 14× smaller than *hashing*.

Next, we compared *HDRF* against two offline partitioning algorithms: *Ginger* and *METIS*. Note that these offline solutions have full knowledge of the input graph that can be exploited to drive their partitioning choices. Figure 3.5b compares the replication factor achieved by these two solutions and *HDRF* (we maintain $|S| = 133$ to be coherent with figure 3.5a). The poor performance of *METIS* was an expected result since it has been proved that edge-cut approaches perform worse than vertex-cut ones on power-law graphs [47]. Moreover, the scope of Metis is to balance vertex load among parts. However, *HDRF* outperforms *Ginger* as well, by reducing its replication factor by 10% on average. In addition, *HDRF* has the clear advantage of consuming the graph in a one-pass fashion while *Ginger* needs several passes over the input data to converge. These results show that *HDRF* is always able to provide a smaller average replication factor with respect to all other algorithms, both streaming and offline.

Figure 3.6 reports the load relative standard deviation produced by the tested streaming algorithms when run on the *MovieLens 10M* dataset with a variable number of target parts (results for other datasets showed similar behavior so we omit them). The curves show that *HDRF* and *greedy* provide the best performance as the number of target parts grows. As expected, *hashing* provides well balanced

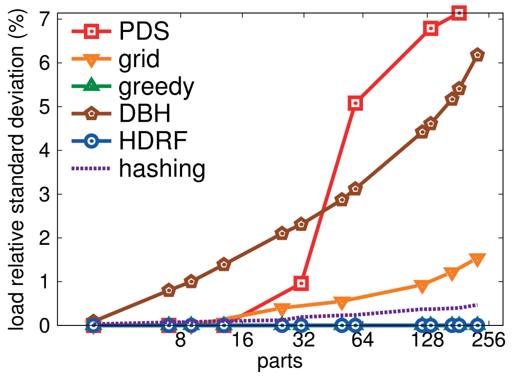

Figure 3.6: Load relative standard deviation produced by different partitioning algorithms on the MovieLens 10M dataset.

parts, but it still performs worse that the other algorithms as its expected behavior with respect to load balancing is only probabilistic. *Grid* performs similarly, even if its more complex constraints induce some skew in load. *DBH* and *PDS* are the worse performers, with load skew growing at a fast pace as the number of target parts grows. Note that replication factor reflects communication cost, and edge-imbalance reflects workload-imbalance; providing good performance with these two metrics means that *HDRF* can provide partitioning results that make the execution of application algorithms more efficient.

To this end, we studied how much all of this translates to a performance improvement with respect to the execution time. To investigate the impact of the different partitioning techniques we ran the GASGD algorithm on GraphLab. Figure 3.7a shows the result of experiments that were run on an EC2 cluster with 31 machines. Figure 3.7b reports the results for the *Tencent Weibo*, with 32, 64 and 128 parts respectively, using a cluster of eight machines. Both figures report the measured speed-up, obtained by using *HDRF* to

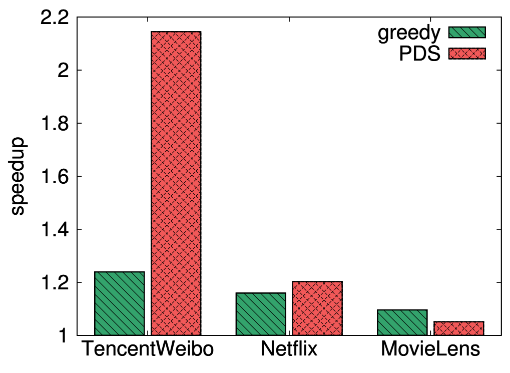

(a) *HDRF*'s speedup with respect to *greedy* and *PDS*, with 32 parts in a 32 machines EC2 cluster.

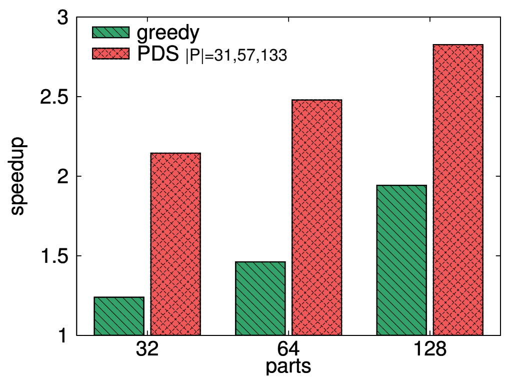

(b) *Tencent Weibo* dataset. *HDRF*'s speedup with respect to *greedy* and *PDS*, with 32, 64 and 128 parts, in a 8 machines cluster.

Figure 3.7: Speedup in the execution time for the GASGD algorithm.

partition the input over *greedy* and *PDS*.[9] The SGD algorithm runs up to two times faster using *HDRF* as input partitioner with respect to *greedy*, and close to three times faster than *PDS*. The actual improvement is larger as the number of target parts grows. Moreover, the speedup is proportional to the gain in RF (see figure 3.4a) and, as already shown in [47], halving the replication factor approximately halves runtime.

Furthermore, having parts with fewer replicas also help GASGD to converge faster. Figure 3.8 shows the trend on the loss (Eq. 2.1) with respect to epoch passing. By using *HDRF* as input partitioner, the GASGD algorithm approaches a minimum with less (or equal) epochs, than using *greedy* or *PDS*, for all the considered datasets.

To recap, HDRF brings a double benefit when using as input partitioner by GASGD: (1) the execution time is faster (using a fixed number of iterations), (2) the convergence needs less epochs. This

[9]We needed to use respectively 31, 57 and 133 parts, to fit *PDS* constraints.

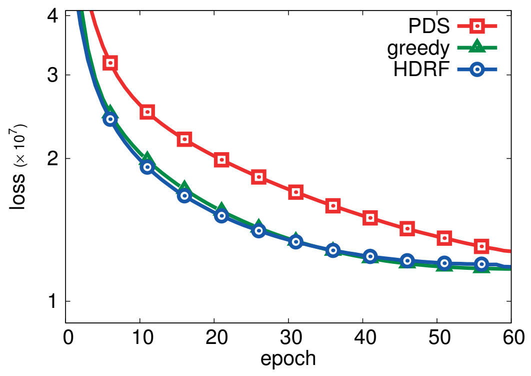

(a) Tencent Weibo

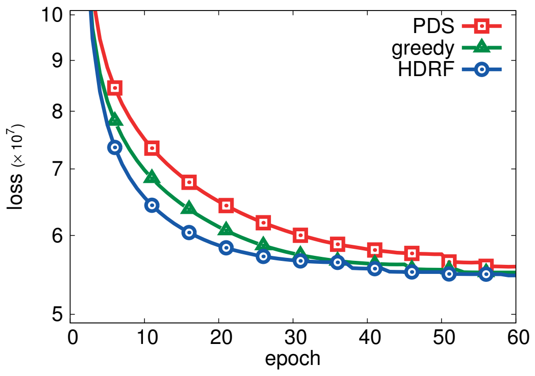

(b) Netflix

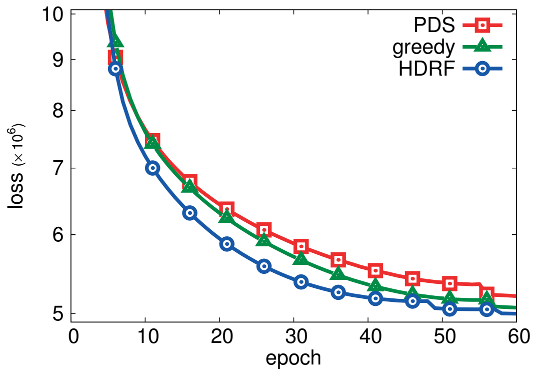

(c) MovieLens 10M

Figure 3.8: Convergence.

means that the execution time can be further reduced by cutting the number of iterations, for instance using some convergence criterion (e.g., stop training when the difference of loss between two subsequent epochs is below a given threshold).

Graph Analytics Runtime

We also studied the performance improvement that HDRF brings to general graph analytics algorithms, namely Single Source Shortest Path (SSSP), Weakly Connected Components (WCC), HCC [57]

algorithm	cpu	network
SSSP	low	low
WCC	low	medium
HCC	low	medium
PR	medium	high
GASGD	high	high

Table 3.3: Algorithms used when measuring execution time with different input graphs.

and Page Rank (PR). Table 3.3 provides more information on the algorithms in terms of cpu and network resource usage. Here, clearly, the tested application algorithm plays an important role: some algorithms may concentrate computation on high-degree nodes while others may place a uniform load on the input graph. In these cases, we expect different improvements. However, the reduction in synchronization overhead among replicas induced by a smaller average replication factor shall in any case positively impact performance. These experiments were run on an EC2 cluster with 31 machines running GraphLab.

Figure 3.9 reports the replication factor for the *twitter-2010*, *uk-2002* and *arabic-2005* datasets. In all our tests *HDRF* outperforms competing solutions.

Figure 3.10 reports the measured speed-up of graph analytics algorithms, obtained by using *HDRF* to partition the input over *greedy* (figure 3.10a) and *PDS* (figure 3.10b). The results confirmed our intuitions: the speedup is proportional to both the advantage in replication factor and the actual network usage of the algorithm. The speedup it is larger for IO-intensive algorithms (e.g., GASGD

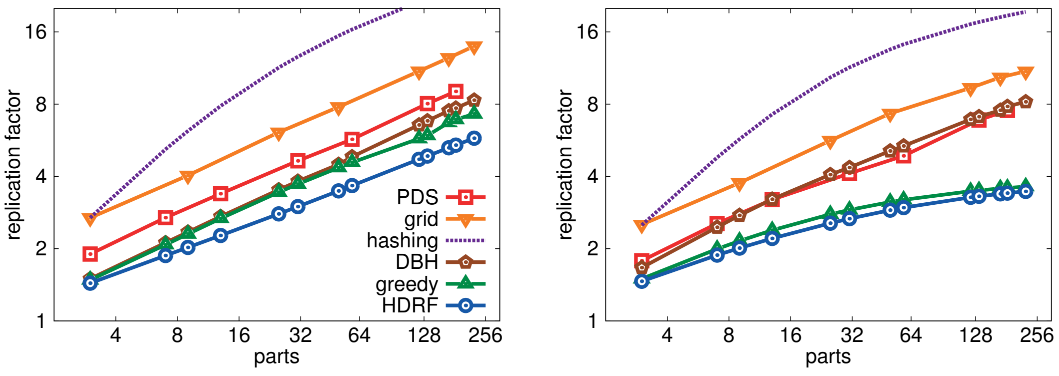

(a) twitter-2010 (b) uk-2002

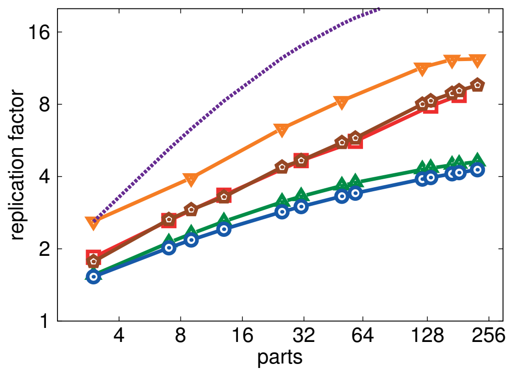

(c) arabic-2005

Figure 3.9: Replication factor varying the number of target parts (log-log scale).

and PR) and smaller for algorithm with less network IO (e.g., SSSP and WCC). None of the tests we conducted with *HDRF* showed a slowdown with respect to other solutions.

Our results show that *HDRF* is the best solution to partition input graphs characterized by skewed power-law degree distributions. *HDRF* achieves the smallest replication factor with close to optimal load balance. These two characteristics combined make application algorithms execute more efficiently in the DGC framework.

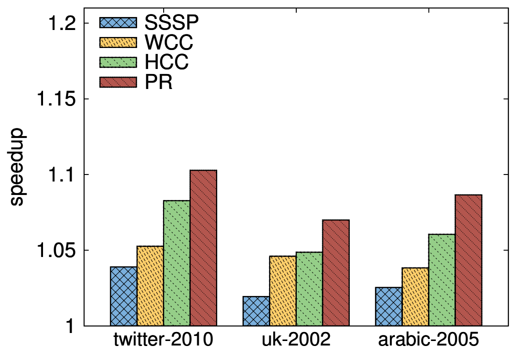

(a) greedy

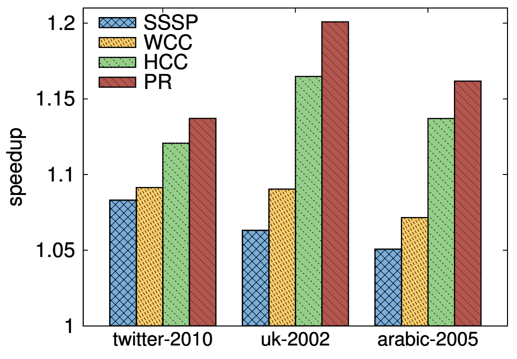

(b) PDS

Figure 3.10: Speedup in the execution time for graph analytics algorithms. Figures show improvements for SSSP, WCC, HCC, and PR, by applying *HDRF* with respect to *greedy* and *PDS* respectively.

Performance sensitivity to input shape

We next analyze how the input graph degree distribution affects *HDRF* performance. To this end, we used *HDRF* to partition a set of synthetic power-law graphs. In doing so, we experimentally characterize the sensitivity of the average replication factor on the power-law shape parameter α, and on the number of parts. Figure 3.11a reports the replication factor improvement for *HDRF* with respect to other algorithms, expressed as a multiplicative factor, by varying α in the range $[1.8, 4.0]$ with $|S| = 128$ target parts ($|S| = 133$ and $|S| = 121$ for *PDS* and *grid* respectively). The curves show two important aspects of *HDRF* behavior: (1) with highly skewed degree distributions (i.e., small values of α), its performance is significantly better than *greedy* and other algorithms (with the exception of DBH); (2) with less skewed degree distributions, the performance of *HDRF* approaches that provided by *greedy*, while all the other solutions (including *DBH*) perform worse. These results show how

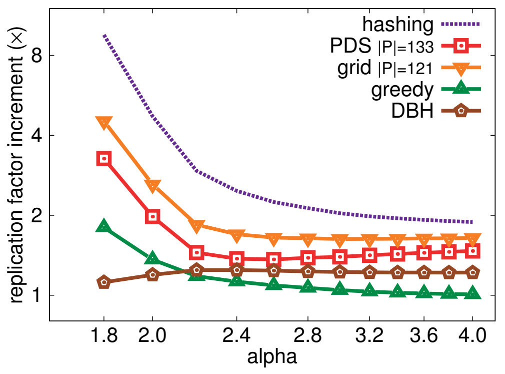

(a) RF increment varying α (*HDRF*$= 1$)

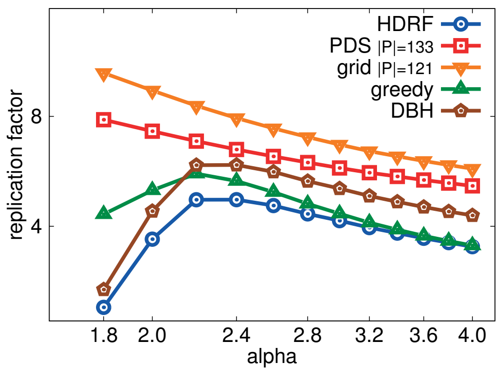

(b) RF varying α

Figure 3.11: Replication factor improvement for *HDRF* in synthetically generated graphs (log-log scale). Figure (a) reports the replication factor increment and figure (b) the actual replication factor when α grows ($|S| = 128$ except for *PDS*, where $|S| = 133$, and *grid*, where $|S| = 121$). For figure (a) *HDRF* represents the baseline.

HDRF behavior approximates *greedy*'s behavior as the number of high degree vertices in the input graph grows as in this case making a different partitioning choice on high-degree vertices is less useful (as there are a lot of them). Note that Gonzalez et al. [47] showed that the effective gain of a vertex-cut approach relative to an edge-cut approach actually increases with smaller α. Our solution boosts this gain, not only with respect to constrained techniques but also over the *greedy* algorithm. Figure 3.11b reports the replication factor, and clearly shows that *HDRF* is able to outperform all competing algorithms for all values of α. At the extremes, *HDRF* is better than *DBH* when α is very small and performs slightly better than *greedy* when α is very large.

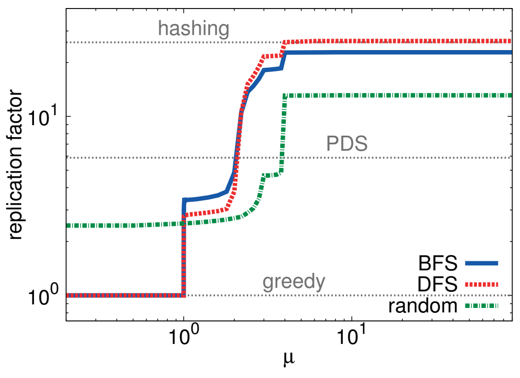

(a) replication factor

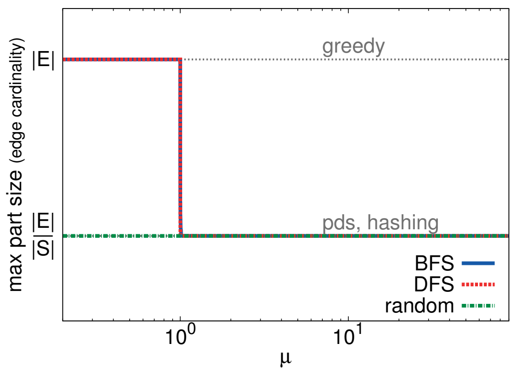

(b) max edge cardinality

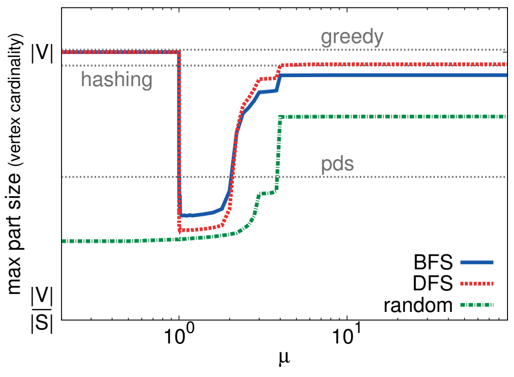

(c) max vertex cardinality

Figure 3.12: *HDRF* behavior on the Netflix dataset varying μ, with input edge stream either random or ordered (DFS or BFS graph visits). Reference grey lines represent *greedy*, *hashing* and *PDS* performance.

Performance sensitivity to input order

A shortcoming of the standard *greedy* algorithm is its inability to effectively handle streaming of input edges when they are ordered. If the algorithm receives the edges ordered such that two subsequent edges always share a vertex, the *greedy* algorithm always places all the edges and their adjacent vertices in a single part. This leads to a degenerate partitioning where, whatever the target parts number is, only a single part holds the whole input graph with the other parts being empty. While this eliminates the need for vertex replicas, the final result is clearly far from being desirable as all of the computation load will be incurred by a single node in the computing cluster.

To overcome this limitation, we explicitly introduced the parameter μ in the computation of the score for each part in *HDRF* (equations (3.6) and (3.8)), that defines the importance of the load balance in the edge placement decision (section 3.2.3). Figure 3.12 shows the result of an experiment run on the Netflix dataset, where the input stream of edges is ordered according to either a *depth-first-search* (DFS) or a *breadth-first-search* (BFS) visit on the graph. The figure shows the average replication factor (figure 3.12a), the size of the largest part expressed as number of contained edges (figure 3.12b) and the size of the largest part expressed as number of contained vertices (figure 3.12c) all while varying the value of μ in the range $[0.1, 100]$ (log-log axes). All three figures report the performance obtained with the *greedy*, *hashing* and *PDS* algorithms as horizontal grey lines for reference.

If we first consider the average replication factor (Figure 3.12a), we can see that as long as $\mu \leq 1$ *HDRF*, the C_{BAL} term in *HDRF*'s cost function is always smaller than 1 and thus makes the algorithm behave exactly as the standard *greedy* algorithm (curves BFS and DFS); all edges are placed in a single part and no vertex is replicated. This behavior is confirmed by the size of the largest part that in this case contains exactly $|E|$ edges and $|V|$ vertices (Figures 3.12b and 3.12c).

For $\mu > 1$, even for values only slightly larger than 1, the C_{BAL} factor starts to play a fundamental role in balancing the load among the available parts: the average replication factor for *HDRF* with both DFS and BFS inputs is just slightly larger than what is achievable with a random input and still substantially lower than what is achievable with *PDS* or *hashing* (figure 3.12a). At the same time, the size of the largest part drops to its minimum (figures 3.12b and 3.12c) indicating that the algorithm immediately delivers close to perfect load balancing (i.e., $|E|/|S|$ edges per part). With these values of μ, the number of vertices hosted in the largest part approaches its theoretical minimum $|V|/|S|$; this value is hypothetical as it is achievable only when the graph is composed of $|S|$ connected components with the same number of vertices. The difference shown by *HDRF* itself when run over a BFS or DFS ordered input with respect to the randomized input can be traced back to our hypothesis that partial information on vertex degrees collected at runtime is a good proxy for the actual degree of the vertices; this hypothesis, in fact, is not true if the input is not randomized: when vertices of the input graph are visited in a non random order, we cannot expect the partitioner to see incoming vertices as a completely uniform random stream. As a consequence, the partial information on vertex degrees can be wrong and drive *HDRF* toward inefficient placement decisions.

By increasing μ toward larger values, the effect of C_{BAL} dominates the *HDRF* cost function; instead of selecting vertices to be replicated on the basis of their degree, the algorithm tries to simply balance parts sizes. In this case, its behavior quickly approaches the behavior typical of the *hashing* algorithm: large average replication factor, with close to perfect load balancing and the largest part containing a number of vertices that approaches $|V|$.

These results show that (1) the C_{BAL} term in *HDRF* score computation plays an effective role in providing close-to-perfect load balancing among parts while keeping a low average replication factor, and (2) by setting the value of μ slightly larger than 1, it is possible to let *HDRF* work at a "sweet spot" where it can deliver the best performance, even when working on an ordered stream of edges. This last point makes *HDRF* particularly suitable for application settings where it is not possible to randomize the input stream before feeding it to the graph partitioning algorithm.

3.4 Summary

Distributed matrix completion algorithms are designed for large scale instances of the problem. Remarkable examples are stratified SGD and asynchronous SGD. For these algorithms, system performance is often determined by the input partitioning strategy, which impacts the communication cost and the workload balance among compute resources. We proposed a transition to a to a graph-based data representation model. This allows to use graph partitioning algorithm to tackle the above challenges.

We proposed *HDRF*, a novel stream-based graph partitioning algorithm. *HDRF* is based on a greedy vertex-cut approach that leverages information on vertex degrees. Through a theoretical analysis and an extensive experimental evaluation on real-world as well as synthetic graphs using both a stand-alone partitioner and implementation of *HDRF* in GraphLab, we showed that HDRF is overall the best performing partitioning algorithm for graphs characterized by power-law degree distributions, that is *HDRF* provides the smallest average replication factor with close to optimal load balance. These two characteristics put together allow *HDRF* to significantly reduce the time needed to perform computation on graphs and makes it the best choice for partitioning graph data. In particular, distributed matrix completion algorithms execute and converge faster when using *HDRF* as input partitioner.

CHAPTER 4

Context-Aware Matrix Completion

Computers are useless. They can only give you answers.

Pablo Picasso

The context in which relationships are observed is an important source of information, whose exploitation can help in the task of understanding and modeling them, therefore to the ultimate goal of providing better predictions. For example, leveraging the purpose of a travel, a hotel recommender system would provide more accurate accommodation suggestions, targeted to, for instance, business trips rather than holidays. However, incorporating generic contextual information inside a latent factor model is challenging. In the following, we review some of the current context-aware matrix completion techniques, developed mostly to enhance the performance of recommender systems.

4.1 Context-Aware Algorithms

There is a large body of research that aims at extending matrix completion models to include such contextual information, mainly focused on collaborative filtering in recommender systems (see [2, 96, 114] for excellent surveys on this topic). Most of the proposed solutions are customized algorithms that integrate a specific information, such as timestamps [65], user tags [134], geolocations [135], but fail in capturing generic contextual data.,

A remarkable example of a general framework are collective matrix factorization (or joint matrix factorization) models [116, 72], which simultaneously factorize the user-item rating matrix and other matrices containing attributes of both users (e.g., user's gender, age, and hobbies) and items (e.g., category and content). However, such models are unable to consider the information associated with the interaction between user and item, e.g., the rating event.

One way to integrate interaction-associated contextual information is using tensor completion models [61, 58, 101, 82, 112]. Such algorithms add a dimension to the user-item rating matrix with contextual data, creating a tensor, that can be factorized using existing techniques, as, for instance, Candecomp/Parafac [61] or Tucker [58] decompositions. Tensor completion models, however, suffer from limited scalability with respect to the amount of contextual information considered. The computational complexity of such models is, in fact, exponential with the number of contextual variables included in the model, and this hampers their applicability in real-world scenarios.

Factorization machines [100, 97, 98] are currently considered the best solutions for context-aware matrix completion, due to their advantages with respect to both scalability and accuracy. In fact, they solve the scalability issues of tensor completion models, experiencing a linear time complexity in the number of contextual variables considered. Factorization machines associate a latent factor vector with each contextual variable. The innovative idea is to model all iteration between pairs of variables (e.g., users, items and context) with the target (e.g., the rating) using factorized interaction parameters. Such parameters are obtained computing the dot product between the latent factor vectors associated with the two variables in the pair (see below for further details).

All existing solutions for context-aware matrix completion require in input both positive and negative evidence, that is the revealed entries in the data matrix have multiple values, a situation that correspond to the presence of explicit feedback in recommender systems and that can be managed using the regularized squared loss optimization criterion.

In what follows we will show how to integrate contextual information inside a matrix completion model in those cases in which only positive evidence exist in input, that is the revealed entries in the matrix have all the same value, a situation that correspond to the presence of implicit feedback in recommender systems and that can be managed using the Bayesian personalized ranking optimization criterion. To this end, we use, as baseline application scenario, a popular natural language processing task: open relation extraction.

4.2 Open Relation Extraction

New generation algorithms for web information retrieval (IR) make use of a knowledge base (KB) to increase their accuracy. A clear example of this is the Google knowledge graph [117]. The basic idea of these techniques is to match the words in a query to real world entities (e.g., a person, a location, etc.) and use real world connections among these entities to improve the task of providing the user with the proper content s/he was looking for. One popular way to represent such KB is through a graph structure, where entities are connected to each other through relations (ex, "born in", "contained by"). This is the idea, for instance, of the web's linked open data cloud [28, 8, 9], a public accessible KB consisting of over 60 billion known facts. Such structures provide exciting opportunities, not only for IR but also for the entire scientific community. However, despite their size, these KBs are still far from being completed. For instance 75% of the people in Freebase [17] have unknown nationality, the place of birth attribute is missing for 71% of all people [130], and coverage for less common relations is even lower. Moreover, relational data can not only be incomplete but also uncertain, noisy and include false information. Automatic methods for relation extraction are therefore needed in order to fill missing information and remove incorrect facts. These algorithms should not only use the information already present in the KB but also scan the web, extracting new information from natural language text in web pages.

Open relation extraction (open RE) is the task of extracting new facts for a potentially unbounded set of relations from various sources such as knowledge bases or natural language text. The task is closely related to *targeted information extraction* (IE) [80, 122, 78], which aims to populate a knowledge base (KB) with new facts for the KB's relations, such as wasBornIn(Sepp Herberger, Mannheim). However, targeted IE methods are inherently limited to an (often small) set of predefined relations, i.e., they are not "open". The open RE task is also related to *open information extraction* (open IE) [11, 40, 32], which extracts large amounts of surface relations and their arguments from natural language text. In contrast to targeted IE, the goal of open IE is to extract all (or most) relations expressed in natural-language text, whether or not these relations are defined in a KB. The facts obtained by open IE methods are often not disambiguated, i.e., the entities and/or the relation are not linked to a knowledge base; e.g., "criticizes"("Dante", "Catholic Church").[1] Although open IE is a domain-independent approach, the extracted surface relations are purely syntactic and often ambiguous or noisy. Moreover, open IE methods usually do not "predict" facts that have not been explicitly observed in the input data. Open RE combines the above tasks by predicting new facts for an open set of relations. The key challenge in open RE is to reason jointly over the *universal schema* consisting of KB relations and surface relations [104].

4.2.1 Relation Extraction Algorithms

Figure 4.1 presents a taxonomy of existing relation extraction algorithms. The main distinction is between closed and open techniques.

[1]We mark (non-disambiguated) mentions of entities and relations in quotation marks.

Closed relation extraction solutions aim at predicting new facts for a set of predefined relations, usually taken from a KB. Existing methods either reason within the KB itself [43, 85, 36] or leverage large text corpora to learn patterns that are indicative of KB relations [80, 122, 78].

The latter solutions typically make use of *distant supervision*, i.e., they start with a set of seed instances (pairs of entities) for the relations of interest, search for these seed instances in text, learn a relation extractor from the so-obtained training data, and optionally iterate [80, 122, 78].

The former techniques are typically based on *tensor completion* models, which use the available data to learn latent semantic representations of entities (i.e., subjects and objects) and relations in a domain-independent way; the latent representations are subsequently used to predict new facts. Tensor completion models conceptually model the input data as a subject×relation×object tensor, in which non-zero values correspond to input facts. The tensor is factored to construct a new tensor in which predicted facts take large non-zero values. Examples of such tensor factorization models are TripleRank [43], RESCAL [85, 86], or PITF [36]. Tensor factorization models are generally well-suited to reason within a KB because they are able to predict relations between arbitrary pairs of subjects and objects.

Open relation extraction algorithms aim at predicting new facts for an unbounded set of relations, that came from various sources, such that natural language text or knowledge bases. Tensor factorization model are not well-suited for open RE, since these methods suffer from limited scalability with the number of relations as well as from

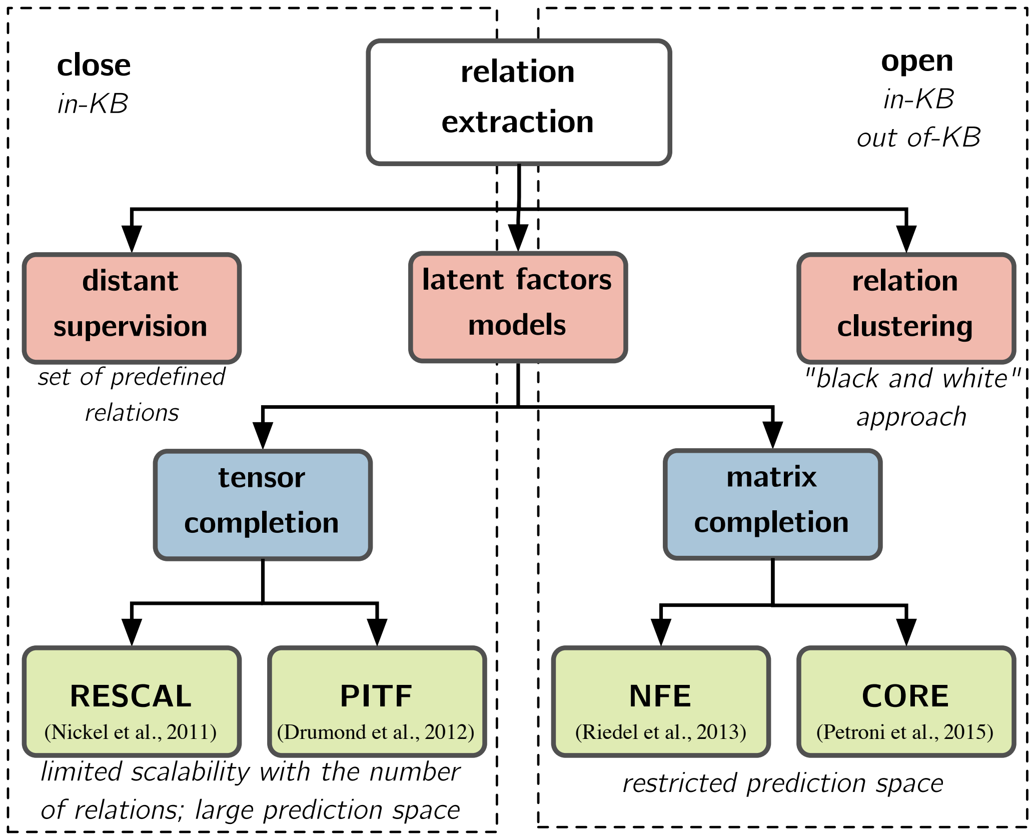
close
in-KB
relation extraction
open
in-KB
out of-KB
distant supervision
set of predefined relations
latent factors models
relation clustering
"black and white" approach
tensor completion
matrix completion
RESCAL (Nickel et al., 2011)
PITF (Drumond et al., 2012)
NFE (Riedel et al., 2013)
CORE (Petroni et al., 2015)
limited scalability with the number of relations; large prediction space
restricted prediction space

Figure 4.1: Taxonomy of relation extraction algorithms.

their large prediction space [22]. In fact, open RE models are more general then targeted IE methods in that they additionally reason about surface relations that do not correspond to KB relations. For this reason, [104] argued and experimentally validated that open RE models can outperform targeted IE methods.

One way to jointly reason about KB and surface relations is to *cluster the relations*: whenever two relations appear in the same cluster, they are treated as synonymous [50, 115, 132, 124, 79, 4, 30]. For example, if “criticizes” and “hates” are clustered together, then we may predict “hates”(“Dante”, “Catholic Church”) from the fact “criticizes"("Dante", "Catholic Church") (which is actually not true). The general problem with relation clustering is its "black and white" approach to relations: either two relations are the same or they are different. This assumption generally does not hold for the surface relations extracted by open IE systems [104]; examples of other types of relationships between relations include implication or mutual exclusion.

Matrix completion approaches try to address the above problem: instead of clustering relations, they directly predict facts, by learning and making use of semantic representations of relations and their arguments. The semantic representations ideally captures all the information present in the data; it does not, however, establish a direct relationship (such as synonymy) between different KB or surface relations. The key difference between matrix and tensor completion models is that the former restrict the prediction space, i.e., these models generally cannot predict arbitrary facts. Similar to distant supervision approaches, matrix completion models focus on predicting facts for which some direct evidence exists. In more detail, most methods restrict the prediction space to the set of facts for which the subject and the object share at least some relation in the input data. For this reason, matrix completion models are not suited for in-KB reasoning; an individual pair of entities usually does not occur in more than one KB relation. In the open RE context, however, input relations are semantically related so that many subject-object pairs belong to multiple relations. The key advantage of matrix methods is (1) that this restriction allows them to use additional features—such as features for each subject-object pair—and (2) that they scale

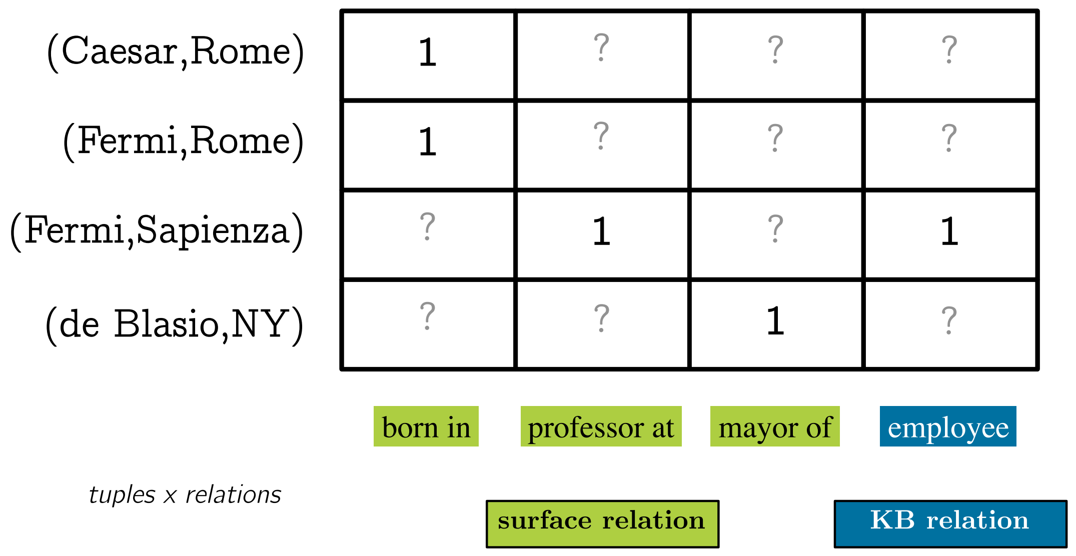

Figure 4.2: Example for representing open RE as a matrix completion problem.

much better with the number of relations. Examples of such matrix factorization models include [126, 55, 104, 41, 53].

Figure 4.2 shows an example for representing open RE as a matrix completion problem. The ones correspond to observed fact, either inside or outside the KB (i.e., containing a surface relation), for instance employee(Fermi,Sapienza) (in-KB) or "mayor of"(de Blasio,NY) (out of-KB). By completing the matrix is possible to estimate the likelihood of missing facts, for instance, in the example, of the fact "mayor of"(Caesar,Rome) or "born in"(de Blasio,NY).

4.3 Context-Aware Open Relation Extraction

CORE [90] is a novel matrix completion model that leverages generic contextual information for open relation extraction. CORE integrates facts from various sources, such as knowledge bases or open information extractors, as well as the context (e.g., metadata about extraction sources, lexical context, or type information) in which these facts have been observed.

Consider for example the sentence "Tom Peloso joined Modest Mouse to record their fifth studio album". Open IE systems may extract the *surface fact* "join"(TP, MM) from this sentence. Note that *surface relation* "join" is unspecific; in this case, it refers to becoming a member of a music band (as opposed to, say, an employee of a company). Most existing open RE systems use the extracted surface fact for further reasoning, but they ignore the context from which the fact was extracted. Actually, exploiting contextual information might be beneficial for open RE. For our example, we may use standard natural language processing tools like a named entity recognizer to detect that TP is a person and MM an organization. These coarse-grained types give us hints about the domain and range of the "join" relation for the surface fact, although the actual meaning of "join" still remains opaque. Now imagine that the above sentence was extracted from a newspaper article published in the music section. This information can help to infer that "join" indeed refers to joining a band. Other contextual information, such as the words "record" and "album" that occur in the sentence, further strengthen this interpretation. A context-aware open RE system should leverage such information to accurately predict facts like "is band member of"(TP, MM) and "plays with"(TP, MM).

Note that the prediction of the fact "is band member of"(TP, MM) is facilitated if we make use of a KB that knows that TP is a musician and MM is a music band. If TP and/or MM are not present in the knowledge base, however, such a reasoning does not apply. In our work, we consider both linked *entities* (in-KB) and non-linked *entity mentions* (out of-KB). Since KB are often incomplete, this open approach to handle named entities allows us to extract facts for all entities, even if they do not appear in the KB.

4.3.1 The CORE Model

Input data. We model the input data as a set of *observations* of the form (r, t, c), where r refer to a KB or surface relation, t refer to a subject-object pair of entities (or entity mentions) and c to contextual information. An observation obtained from the above example may be (“join”, (TP, MM), { types:(person,org), topic:music, word:record, word:album, . . . }). Denote by R the set of all observed *relations*, by E the set of all observed *entities*, and by $T \subseteq E \times E$ the set of all observed entity pairs, which we refer to as *tuples*. A *fact* takes form $r(t)$ and is composed of a relation $r \in R$ and a tuple $t \in T$; e.g., “join”(TP, MM). Note that there may be multiple observations for a fact. Finally, denote by C the set of all *contextual variables*; each observation is associated with a set $c \subseteq C$ of context variables.

Problem definition. The open RE task is to produce a ranked list of tuples $T_r \subseteq T$ for each relation $r \in R$; the list is restricted to new tuples, i.e., tuples $t \in T$ for which $r(t)$ has not been observed in the input. The rank of each tuple reflects the model’s prediction of the likelihood that the corresponding fact is indeed true. A good model thus ranks correct facts higher than incorrect ones.

Symbol	Description
R	Relations set
T	Tuples set
E	Entities set
C	Contextual variables set
T_r	Ranked list of tuples for relation r
V	Variables set; $R \cup T \cup E \cup C$; Columns set
X	Training points; Rows set
d	Dimensionality of the completion; rank of the factorization

Table 4.1: Notation for matrix completion algorithms in open relation extraction.

Modeling facts. Denote by $V = R \cup T \cup E \cup C$ the set of all observed relations, tuples, entities, and contextual variables. For ease of exposition, we refer to the elements of V as *variables*. We model the input data in terms of a matrix in which each row corresponds to a fact (i.e., not an observation) and each column to a variable. We group columns according to the type of the variables; e.g, there are relation columns, tuple columns, entity columns, and a group of columns for each type of contextual information. The matrix is populated such that in each row the values of each column group sum up to unity, i.e., we normalize values within column groups. In particular, we set to 1 the values of the variable of the relation and the tuple of the corresponding fact. We set to 0.5 the variables corresponding to the two entities referred to by the fact.

An example is shown in Fig. 4.3. Here the first row, for instance, corresponds to the fact "born in"(Caesar, Rome). Note that we model tuples and entities separately: the entity variables expose which arguments belong to the fact, the tuple variables expose their order.

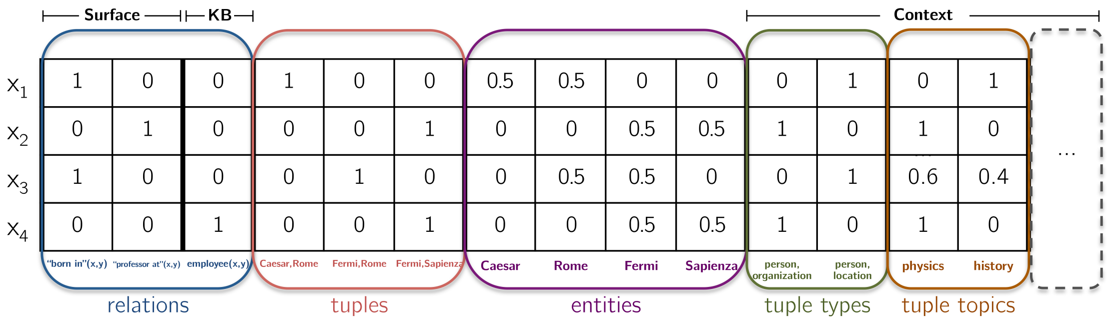

	"born in"(x,y)	"professor at"(x,y)	employee(x,y)	Caesar,Rome	Fermi,Rome	Fermi,Sapienza	Caesar	Rome	Fermi	Sapienza	person, organization	person, location	physics	history
x_1	1	0	0	1	0	0	0.5	0.5	0	0	0	1	0	1
x_2	0	1	0	0	0	1	0	0	0.5	0.5	1	0	1	0
x_3	1	0	0	0	1	0	0	0.5	0.5	0	0	1	0.6	0.4
x_4	0	0	1	0	0	1	0	0	0.5	0.5	1	0	1	0

Figure 4.3: Example for representing a context-aware open RE problem with CORE.

Modeling context. As described above, we model the data in terms of a matrix in which rows corresponds to facts (instead of observations). The reasoning behind this approach is as follows. First, we may see a fact in multiple observations; our goal is to leverage all the available context. Second, facts but not observations are the target of our predictions. Finally, we are interested in predicting new facts, i.e., facts that we have not seen in the input data. For these facts, there is no corresponding observation so that we cannot directly obtain contextual information. To address these points, the CORE model aggregates the context of relevant observations for each fact; this approach allows us to provide comprehensive contextual information for both observed and unobserved facts.

We group contextual information by the type of information: examples include metadata about the extraction sources (e.g., from an article on music), types of the entities of a tuple (e.g., (person, location)), or the bag-of-words in the sentence from which an extraction has been obtained. We aggregate the contextual information for each tuple $t \in T$; this tuple-level approach allows us to provide contextual information for unobserved facts. In more detail, we count in how many observations each contextual variable has been associated with the tuple, and then normalize the count values to 1 within each group of columns. The so-obtained values can be interpreted as the relative frequencies with which each contextual variable is associated with the tuple. The contextual information associated with each fact is given by the aggregated, normalized context of its tuple.

Fig. 4.3 shows context information arranged in two groups: tuple types and tuple topics. We capture information such as that the tuple (Caesar, Rome) has only been seen in articles on history or that tuple (Fermi, Rome) is mentioned in both physics and history articles (slightly more often in the former). Since context is associated with tuples, facts 2 and 4 on (Fermi, Sapienza) share contextual information. This form of context sharing (as well as entity sharing) allows us to propagate information about tuples across various relations.

Factorization model. CORE employs a matrix completion model based on factorization machines and the open-world assumption to capture latent semantic information about the individual variables. In particular, we associate with each variable $v \in V$ a *bias term* $b_v \in \mathbb{R}$ and a *latent feature vector* $\boldsymbol{f}_v \in \mathbb{R}^d$, where the *dimensionality* d of the latent feature space is a hyperparameter of the model. Denote by X the set of rows in the input matrix, which we henceforth refer to as *training points*. For each training point $x \in X$, denote by x_v the value of variable $v \in V$ in the corresponding row of the matrix. Our model associates with training point $x \in X$ a *score* $s(x)$ computed as follows:

$$s(x) = \sum_{v \in V} x_v b_v + \sum_{v_1 \in V} \sum_{v_2 \in V \setminus \{v_1\}} x_{v_1} x_{v_2} \boldsymbol{f}_{v_1}^T \boldsymbol{f}_{v_2} \tag{4.1}$$

Here the bias terms model the contribution of each individual variable to the final score, whereas the latent feature vectors model the contribution of all pairwise interactions between variables. Note that only bias terms and feature vectors corresponding to non-zero entries in x affect the score and that x is often sparse. Since we can compute $s(x)$ in time linear to both the number of nonzero entries in x and the dimensionality d [97], score computation is fast. As discussed below, we (roughly) estimate bias terms and feature vectors such that observed facts achieve high scores. We may thus think of each feature vector as a low-dimensional representation of the global information contained in the corresponding variable.

Prediction. Given estimates for bias terms and latent feature vectors, we rank unobserved facts as follows. Fix a relation $r \in R$ and a tuple $t \in T$ such that $r(t)$ has not been observed. As indicated above, the CORE model overcomes the key problem that there is no observation, and thus no context, for $r(t)$ by context aggregation and sharing. In particular, we create an *test point* $\hat{x}$ for tuple $r(t)$ in a way similar to creating data points, i.e., we set the relation, tuple, and entity variables accordingly and add the aggregated, normalized context of t. Once test point $\hat{x}$ has been created, we can predict its score $s(\hat{x})$ using Eq. (4.1). We then rank each unobserved tuple by its so-obtained score, i.e., tuples with higher scores are ranked higher. The resulting ranking constitutes the list T_r of predicted facts for relation r.

Bayesian personalized ranking. The parameters of the CORE model are given by $\Theta = \{\, b_v, \boldsymbol{f}_v \mid v \in V \,\}$. In approaches based on the closed-world assumption, Θ is estimated by minimizing the error between model predictions and target values (e.g., 1 for true facts, 0 for false facts). In our setting of open RE, all our observations are positive, i.e., we do not have negative training data. One way to handle the absence of negative training data is to associate a target value of 0 to all unobserved facts. This closed-world approach essentially assumes that all unobserved facts are false, which may not be a suitable assumption for the sparsely observed relations of open RE. Following [104], we adopt the open-world assumption instead, i.e., we treat each unobserved facts as unknown. Since factorization machines originally require explicit target values (e.g., feedback in recommender systems), we need to adapt parameter estimation to the open-world setting.

In more detail, we employ a variant of the Bayesian personalized ranking (BPR) optimization criterion [99]. We associate with each training point x a set of *negative samples* X_x^-. Each negative sample $x^- \in X_x^-$ is an unobserved fact with its associated context (constructed as described in the prediction section above). Generally, the negative samples x^- should be chosen such that they are "less likely" to be true than fact x. We maximize the following optimization criterion:

$$\frac{1}{|X|}\sum_{x\in X}\left(\sum_{x^-\in X_x^-}\frac{\ln\sigma(\delta(x,x^-))}{|X_x^-|}-\lambda\|\Theta_x\|^2\right) \tag{4.2}$$

where $\sigma(x)=\frac{1}{1+e^{-x}}$ denotes the logistic function, $\delta(x,x^-)=s(x)-s(x^-)$ denotes the difference of scores, and $\Theta_x=\{\,b_v,\boldsymbol{f}_v\mid x_v\neq 0\,\}$ the subset of the model parameters relevant for training point x. Here we use L2 regularization controlled by a single hyperparameter λ. In essence, the BPR criterion aims to maximize the average "difference" $\ln\sigma(\delta(x,x^-))$ between the score of fact x and each of its negative samples x^-, averaged over all facts. In other words, we aim to score x higher than each x^-. (Note that under the closed-world assumption, we would instead consider x^- as being false.) For a more in-depth discussion of BPR, see [99].

Sampling negative evidence. To make BPR effective, the set of negative samples needs to be chosen carefully. A naive approach is to take the set of all unobserved facts between each relation $r\in R$ and each tuple $t\in T$ (or $E\times E$) as the set X_x^-. The reasoning is that, after all, we expect "random" unobserved facts to be less likely to be true than observed facts. This naive approach is problematic, however, because the set of negative samples is independent of x and thus not sufficiently informative (i.e., it contains many irrelevant samples).

To overcome this problem, the negative sample set needs to be related to x in some way. Since we ultimately use the model to rank tuples for each relation individually, we consider as negative evidence for x only unobserved facts from the same relation [104]. In more detail, we (conceptually) build a negative sample set X_r^- for each relation $r \in R$. We include into X_r^- all facts $r(t)$—again, along with their context—such that $t \in T$ is an observed tuple but $r(t)$ is an unobserved fact. Thus the subject-object pair t of entities is not observed with relation r in the input data (but with some other relation). The set of negative samples associated with each training point x is defined by the relation r of the fact contained in x, that is $X_x^- = X_r^-$. Note that we do not actually construct the negative sample sets; see below.

Parameter estimation. We maximize Eq. (4.2) using stochastic gradient ascent. This allows us to avoid constructing the sets X_x^-, which are often infeasibly large, and worked well in our experiments. In particular, in each stochastic gradient step, we randomly sample a training point $x \in X$, and subsequently randomly sample a negative sample $x^- \in X_x^-$. This sampling procedure can be implemented very efficiently. We then perform the following ascent step with learning rate η:

$$\Theta \leftarrow \Theta + \eta \nabla_\Theta \left(\ln \sigma(\delta(x, x^-)) - \lambda \|\Theta_x\|^2 \right)$$

One can show that the stochastic gradient used in the formula above is an unbiased estimate of the gradient of Eq. (4.2). To speed up parameter estimation, we use a parallel lock-free version of stochastic gradient ascent as in [95]. This allows the CORE model to handle (reasonably) large datasets.

	size	info
facts	453.9k	14.7k Freebase, 174.1k surface linked, 184.5k surface partially-linked, 80.6k surface non-linked.
relations	4.7k	94 Freebase, 4.6k surface.
tuples	178.5k	69.5k linked, 71.5k partially-linked, 37.5k non-linked.
entities	114.2k	36.8k linked, 77.4k non-linked.

Table 4.2: Dataset statistics.

4.4 Evaluation

We conducted an experimental study on real-world data to compare the CORE model with other state-of-the-art approaches.[2] Our experimental study closely follows the one of [104].

4.4.1 Experimental Setup

Dataset. We made use of the dataset of [104], but extended it with contextual information. The dataset consisted of 2.5M surface facts extracted from the New York Times corpus [107], as well as 16k facts from Freebase [17]. Surface facts have been obtained by using a named-entity recognizer, which additionally labeled each named entity mention with its coarse-grained type (i.e., person, organization, location, miscellaneous). For each pair of entities found within

[2]Source code, datasets, and supporting material are available at `https://github.com/fabiopetroni/CORE`

a sentence, the shortest dependency path between these pairs was taken as surface relation. The entity mentions in each surface fact were linked to Freebase using a simple string matching method. If no match was found, the entity mention was kept as is. There were around 2.2M tuples (distinct entity pairs) in this dataset, out of which 580k were fully linked to Freebase. For each of these tuples, the dataset additionally included all of the corresponding facts from Freebase. Using the metadata[3] of each New York Times article, we enriched each surface fact by the following contextual information: news desk (e.g., sports desk, foreign desk), descriptors (e.g., finances, elections), online section (e.g., sports, business), section (e.g., a, d), publication year, and bag-of-words of the sentence from which the surface fact has been extracted.

Training data. From the raw dataset described above, we filtered out all surface relations with less than 10 instances, and all tuples with less than two instances, as in [104]. Tab. 4.2 summarizes statistics of the resulting dataset. Here we considered a fact or tuple as *linked* if both of its entities were linked to Freebase, as *partially-linked* if only one of its entities was linked, and as *non-linked* otherwise. In contrast to previous work [104, 22], we retain partially-linked and non-linked facts in our dataset.

Evaluation set. Open RE models produce predictions for all relations and all tuples. To keep the experimental study feasible and comparable to previous studies, we use the full training data but evaluate each model's predictions on only the subsample of 10k tuples ($\approx 6\%$ of all tuples) of [104]. The subsample consisted of 20%

[3]Further information can be found at `https://catalog.ldc.upenn.edu/LDC2008T19`.

linked, 40% partially-linked and 40% non-linked tuples. For each (surface) relation and method, we predicted the top-100 new facts (not in training) for the tuples in the subsample.

Considered methods. We compared various forms of the CORE model with PITF and the matrix factorization model NFE. Our study focused on these two factorization models because they outperformed other models (including non-factorization models) in previous studies [104, 22]. All models were trained with the full training data described above.

PITF [36]. PITF is a recent tensor factorization method designed for within-KB reasoning. PITF is based on factorization machines so that we used our scalable CORE implementation for training the model.

NFE [104]. NFE is the full model proposed in the "universal schema" work of [104]. It uses a linear combination of three component models: a neighborhood model (N), a matrix factorization model (F), and an entity model (E). The F and E models together are similar (but not equal) to the CORE model without context. The NFE model outperformed tensor models [22] as well as clustering methods and distantly supervised methods in the experimental study of [104] for open RE tasks. We use the original source code of [104] for training.

CORE. We include multiple variants of the model in the experimental study, each differing by the amount of context being used. We consider as context the article metadata (m), the tuple types (t) and the bag-of-words (w). Each tuple type is a pair of subject-object types of (e.g. (person, location)). The basic CORE model uses relations, tuples and entities as variables. We additionally consider the CORE+t, CORE+w, CORE+mt, and CORE+mtw models, where the suffix indicates which contextual information has been included. The total number of variables in the resulting models varied between 300k (CORE) to 350k (CORE+mtw). We used a modified version of *libfm* for training.[4] Our version adds support for BPR and parallelizes the training algorithm.

Methodology. To evaluate the prediction performance of each method, we followed [104]. We considered a collection of 19 Freebase relations (Tab. 4.3) and 10 surface relations (Tab. 4.4) and restrict predictions to tuples in the evaluation set.

Evaluation metrics. For each relation and method, we computed the top-100 evaluation set predictions and labeled them manually. We used as evaluation metrics the mean average precision defined as:

$$\text{MAP}_{\#}^{100} = \frac{\sum_{k=1}^{100} I_k \cdot P@k}{\min\{100, \#\}} \tag{4.3}$$

where indicator I_k takes value 1 if the k-th prediction is true and 0 otherwise, and # denotes the number of true tuples for the relation in the top-100 predictions of all models. The denominator is included to account for the fact that the evaluation set may include less than 100 true facts. $\text{MAP}_{\#}^{100}$ reflects how many true facts are found by each method as well as their ranking. If all # facts are found and ranked top, then $\text{MAP}_{\#}^{100} = 1$. Note that this definition

[4]the surce code is available at `https://github.com/fabiopetroni/libfm`

of $\text{MAP}_{\#}^{100}$ differs slightly from [104]; this metric is more robust because it is based on completely labeled evaluation data. To compare the prediction performance of each system across multiple relations, we averaged $\text{MAP}_{\#}^{100}$ values, in both an unweighted and a weighted (by #) fashion.

Parameters. For all systems, we used $d = 100$ latent factors, $\lambda = 0.01$ for all variables, a constant learning rate of $\eta = 0.05$, and ran 1000 epochs of stochastic gradient ascent. These choices correspond to the ones of [104]; no further tuning was performed.

4.4.2 Results

Prediction performance. The results of our experimental study are summarized in table 4.3 (Freebase relations) and table 4.4 (surface relations). As mentioned before, all reported numbers are with respect to our evaluation set. Each entry shows the number of true facts in the top-100 predictions and, in parentheses, the $\text{MAP}_{\#}^{100}$ value. The # column list the total number of true facts found by at least one method. The last two lines show the aggregated $\text{MAP}_{\#}^{100}$ scores.

We start our discussion with the results for Freebase relations (table 4.3 and figure 4.4). First note that the PITF model generally did not perform well; as discussed before, tensor factorization models such as PITF suffer from a large prediction space and cannot incorporate tuple-level information. NFE and CORE, both matrix factorization models, performed better and were on par with each other. This indicates that the use of factorization machines does not

Relation	#	PITF	NFE	CORE	CORE+m	CORE+t	CORE+w	CORE+mt	CORE+mtw
person/company	208	70 (0.47)	92 (0.81)	91 (0.83)	90 (0.84)	91 (0.87)	92 (0.87)	95 (0.93)	**96** (**0.94**)
person/place_of_birth	117	1 (0.0)	92 (*0.9*)	90 (0.88)	92 (*0.9*)	92 (*0.9*)	89 (0.87)	**93** (*0.9*)	92 (*0.9*)
location/containedby	102	7 (0.0)	63 (0.47)	62 (0.47)	63 (0.46)	61 (0.47)	61 (0.44)	62 (0.49)	**68** (**0.55**)
parent/child	88	9 (0.01)	64 (0.6)	64 (0.56)	64 (0.59)	64 (0.62)	64 (0.57)	67 (**0.67**)	**68** (0.63)
person/place_of_death	71	1 (0.0)	67 (0.93)	67 (0.92)	*69* (*0.94*)	67 (0.93)	67 (0.92)	*69* (*0.94*)	67 (0.92)
person/parents	67	20 (0.1)	51 (0.64)	52 (0.62)	51 (0.61)	49 (0.64)	47 (0.6)	*53* (**0.67**)	*53* (0.65)
author/works_written	65	24 (0.08)	45 (0.59)	49 (0.62)	51 (0.69)	50 (0.68)	50 (0.68)	51 (**0.7**)	**52** (0.67)
person/nationality	61	21 (0.08)	25 (0.19)	27 (0.17)	28 (0.2)	26 (0.2)	**29** (0.19)	27 (0.18)	27 (**0.21**)
neighbor./neighborhood_of	39	3 (0.0)	24 (0.44)	23 (0.45)	26 (0.5)	27 (0.47)	27 (0.49)	*30* (0.51)	*30* (**0.52**)
film/directed_by	15	7 (0.06)	7 (0.15)	11 (0.22)	9 (0.25)	10 (0.27)	**15** (**0.52**)	11 (0.28)	12 (0.31)
company/founders	11	0 (0.0)	*10* (*0.34*)	*10* (*0.34*)	*10* (0.26)	*10* (0.21)	*10* (0.22)	*10* (0.22)	*10* (0.24)
sports_team/league	11	1 (0.0)	7 (0.24)	*10* (0.23)	*10* (*0.3*)	7 (0.22)	*10* (0.27)	8 (0.29)	9 (*0.3*)
structure/architect	11	7 (0.63)	7 (0.63)	9 (0.7)	*11* (0.84)	*11* (0.73)	*11* (**0.9**)	*11* (0.8)	10 (0.77)
team/arena_stadium	9	2 (0.01)	6 (0.14)	6 (0.19)	6 (0.18)	6 (0.15)	6 (0.18)	*7* (**0.29**)	*7* (0.2)
team_owner/teams_owned	9	4 (0.05)	6 (0.17)	7 (0.18)	7 (0.33)	6 (0.27)	7 (0.19)	6 (0.22)	**8** (**0.34**)
film/produced_by	8	1 (0.03)	4 (0.06)	3 (0.13)	2 (0.12)	3 (0.03)	*6* (0.09)	3 (0.13)	*6* (**0.15**)
roadcast/area_served	5	0 (0.0)	4 (0.71)	4 (**0.73**)	4 (0.65)	4 (0.66)	4 (0.66)	*5* (0.64)	*5* (0.72)
person/religion	5	2 (0.0)	*3* (0.21)	2 (0.22)	1 (0.2)	*3* (0.22)	*3* (**0.25**)	2 (0.21)	*3* (0.21)
composer/compositions	3	*2* (0.1)	*2* (0.34)	*2* (0.35)	*2* (0.34)	*2* (0.35)	1 (0.33)	*2* (0.22)	*2* (**0.36**)
Average $\text{MAP}_{\#}^{100}$		0.09	0.46	0.47	0.49	0.47	0.49	0.49	**0.51**
Weighted Average $\text{MAP}_{\#}^{100}$		0.14	0.64	0.64	0.66	0.67	0.66	*0.70*	*0.70*

Table 4.3: True facts and $\text{MAP}_{\#}^{100}$ (in parentheses) in the top-100 evaluation-set tuples for Freebase relations. We consider as context the article metadata (m), the tuple types (t) and the bag-of-words (w). Best value per relation in bold (unique winner) or italic (multiple winners). Average weighs are # column values.

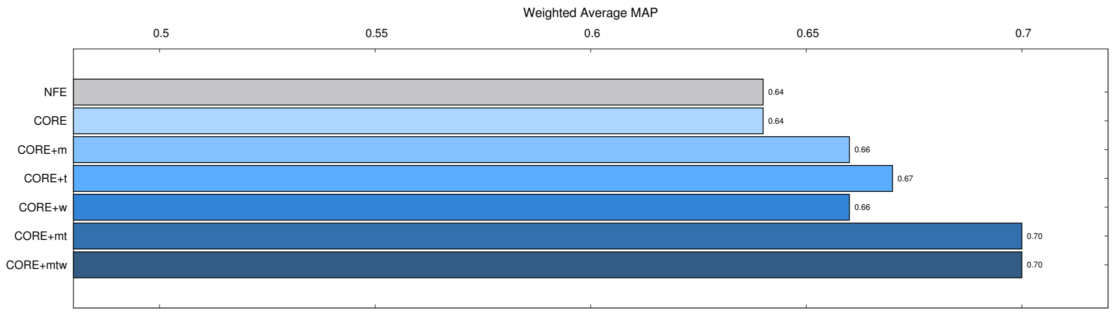

Figure 4.4: Weighted Average $\text{MAP}_{\#}^{100}$ for Freebase relations

affect performance in the absence of context; after all, both methods essentially make use of the same amount of information. The key advantage of CORE over NFE is that we can incorporate contextual information. Our results indicate that using such information indeed improves prediction performance. The CORE+mtw model

Relation	#	PITF	NFE	CORE	CORE+m	CORE+t	CORE+w	CORE+mt	CORE+mtw
head	162	34 (0.18)	80 (0.66)	83 (0.66)	82 (0.63)	76 (0.57)	77 (0.57)	83 (0.69)	**88** (**0.73**)
scientist	144	44 (0.17)	76 (0.6)	74 (0.55)	73 (0.56)	74 (0.6)	73 (0.59)	*78* (0.66)	*78* (**0.69**)
base	133	10 (0.01)	85 (0.71)	86 (0.71)	86 (0.78)	88 (0.79)	85 (0.75)	83 (0.76)	**89** (**0.8**)
visit	118	4 (0.0)	73 (0.6)	75 (0.61)	76 (0.64)	80 (0.68)	74 (0.64)	75 (0.66)	**82** (**0.74**)
attend	92	11 (0.02)	65 (0.58)	64 (0.59)	65 (0.63)	62 (0.6)	66 (0.63)	62 (0.58)	**69** (**0.64**)
adviser	56	2 (0.0)	42 (0.56)	**47** (0.58)	44 (0.58)	43 (0.59)	45 (*0.63*)	43 (0.53)	44 (*0.63*)
criticize	40	5 (0.0)	31 (0.66)	33 (0.62)	33 (**0.7**)	33 (0.67)	33 (0.61)	35 (0.69)	**37** (0.69)
support	33	3 (0.0)	19 (0.27)	22 (*0.28*)	18 (0.21)	19 (*0.28*)	22 (0.27)	**23** (0.27)	21 (0.27)
praise	5	0 (0.0)	2 (0.0)	2 (0.01)	4 (*0.03*)	3 (0.01)	3 (0.02)	**5** (*0.03*)	2 (0.01)
vote	3	2 (0.01)	*3* (0.63)	*3* (0.63)	*3* (0.32)	*3* (0.49)	*3* (0.51)	*3* (0.59)	*3* (**0.64**)
Average $\text{MAP}_{\#}^{100}$		0.04	0.53	0.53	0.51	0.53	0.53	0.55	**0.59**
Weighted Average $\text{MAP}_{\#}^{100}$		0.08	0.62	0.61	0.63	0.63	0.61	0.65	**0.70**

Table 4.4: True facts and $\text{MAP}_{\#}^{100}$ (in parentheses) in the top-100 evaluation-set tuples for surface relations. We consider as context the article metadata (m), the tuple types (t) and the bag-of-words (w). Best value per relation in bold (unique winner) or italic (multiple winners). Average weighs are # column values.

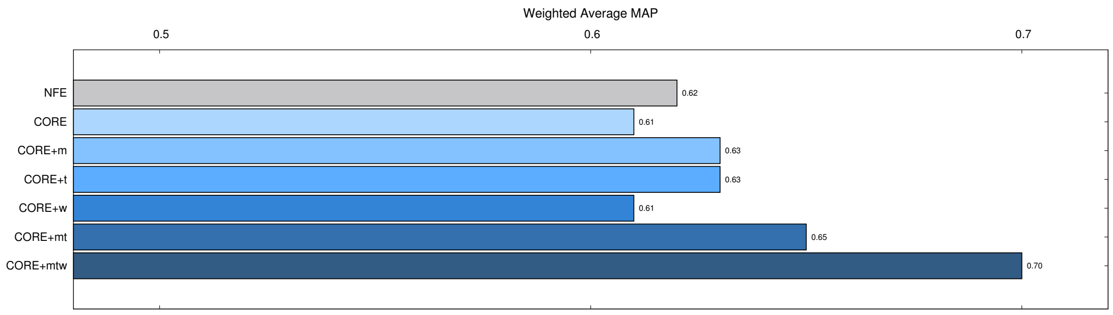

Figure 4.5: Weighted Average $\text{MAP}_{\#}^{100}$ for surface relations

performed best overall; it increased the average $\text{MAP}_{\#}^{100}$ by four points (six points weighted) compared to the best context-unware model. Note that for some relations, including only subsets of the contextual information produced better results than using all contextual information (e.g., film/directed_by). We thus conjecture that extending the CORE model by variable-specific regularization terms may be beneficial.

Table 4.4 and figure 4.5 summarize our results for surface relations. In general, the relative performance of the models agreed with the author(x,y)

ranked list of tuples	similar relations
1 (Winston Groom, Forrest Gump)	0.98 "reviews x by y"(x,y)
2 (D. M. Thomas, White Hotel)	0.97 "book by"(x,y)
3 (Roger Rosenblatt, Life Itself)	0.95 "author of"(x,y)
4 (Edmund White, Skinned Alive)	0.95 " 's novel"(x,y)
5 (Peter Manso, Brando: The Biography)	0.95 " 's book"(x,y)
6 (Edward J. Renehan Jr., The Lion's Pride)	0.91 "who wrote"(x,y)
7 (Richard Taruskin, Stravinsky and ...)	0.89 " 's poem"(x,y)
...	...

"scientist at"(x,y)

ranked list of tuples	similar relations
1 (Riordan Roett, Johns Hopkins University)	0.87 "scientist"(x,y)
2 (Dr. R. M. Roberts, University of Missouri)	0.84 "scientist with"(x,y)
3 (Linda Mayes, Yale University)	0.80 "professor at"(x,y)
4 (Daniel T. Jones, Cardiff Business School)	0.79 "scientist for"(x,y)
5 (Russell Ross, University of Iowa)	0.78 "neuroscientist at"(x,y)
6 (Eva Richter, Kingsborough College)	0.76 "geneticist at"(x,y)
7 (M.L. Weidenbaum, Washington University)	0.75 "physicist at"(x,y)
...	...

Figure 4.6: Some facts predicted by the CORE+mtw model for the Freebase relation author(x,y) and the surface relation "scientist at"(x,y). Most similar relations also reported, using cosine similarity between the corresponding latent feature vectors as distance.

one on Freebase relations. One difference is that using bag-of-word context significantly boosted prediction performance. One reason for this boost is that related surface relations often share semantically related words (e.g., "professor at" and "scientist at") and may occur in similar sentences (e.g., mentioning "university", "research", ...).

Anecdotal results. Fig. 4.6 shows the top test-set predictions of CORE+mtw for the author and "scientist at" relations. In both cases, we also list relations that have a similar semantic representation in the CORE model (highest cosine similarity). Note that semantic similarity of relations is one aspect of the model; predictions incorporate other aspects such as context (i.e., two “similar” relations in different contexts are treated differently).

Training time. We used a machine with 16-cores Intel Xeon processor and 128GB of memory. Training CORE took roughly one hour, NFE roughly six hours (single core only), and training CORE+mtw took roughly 20 hours. Our implementation can handle reasonably large data, but an investigation of faster, more scalable training methods appears worthwhile.

4.5 Summary

Context-aware matrix completion aims at integrating additional information inside the model, in order to increase the overall prediction performance. In this chapter we presented current solutions for this task, and extended them in order to work in those settings in which only positive observations are present in input, using relation extraction as application scenario.

In particular, we presented CORE, a matrix completion model for open relation extraction that incorporates contextual information. Our model is based on factorization machines and the open-world assumption, integrates various forms of contextual information, and is extensible, i.e., additional contextual information can be integrated when available. Our experimental study on a large real-world dataset indicates that CORE has significantly better prediction performance than state-of-the-art relation extraction approaches when contextual information is available.

CHAPTER 5

Conclusion and Outlook

Prediction is very difficult, especially about the future.

Niels Bohr

In this thesis, we addressed efficient solutions for large-scale matrix completion problems based on latent factor models. We worked over two lines, respectively tackling the scalability of such solutions and their prediction quality.

To handle large-scale instances of the matrix completion problem, asynchronous algorithms based on latent factor models have been proposed. Such solutions distribute the input over a cluster of computing nodes, that can communicate asynchronously, and then perform the training procedure in a distributed fashion. In order to achieve a fast execution time, a key challenge is to minimize the communication between computing nodes while balancing the workload. With this aim, we proposed GASGD, a variant of the asynchronous stochastic gradient descend algorithm that represents the data matrix as a graph. This allows GASGD to make use of graph partitioning algorithms for the distributed placement of the input. As partitioning solution, we proposed *HDRF*, a novel vertex-cut stream-based graph partitioning algorithm that exploits a common characteristic of real graphs to improve the performance, that is their power-law degree distribution. The distributed matrix completion procedure is more scalable when using *HDRF* to partition the input data, since it experiments less data overlap among the computing nodes, hence the communication in the system is reduced. It is also more efficient, since computing nodes receive almost perfectly equal slices of the input to process. Our empirical studies on real and synthetic datasets showed the effectiveness of this approach, in that the distributed asynchronous stochastic gradient descent algorithm proved to converge and run faster when using *HDRF* as input partitioner. We also provided a theoretical study for the *HDRF* algorithm and an analysis of its behavior when applied on general graph computation algorithms.

Several studies have shown that feeding the algorithm with more data might be beneficial for the overall prediction quality of the system. To further improve the performance, it is necessary to somehow incorporate contextual information inside the model, that helps (even as humans) the refining of the input data. However incorporating such information in the model, especially when the system detects only positive evidence in input, that is when the revealed entries in the data matrix have all the same value, is a challenging task. We proposed a latent factor based matrix completion model than can exploit contextual information even in the above case, using as prototypical application scenario a popular natural language processing task: relation extraction. In particular, we proposed CORE, a novel context-aware matrix completion solution for open relation extraction. Our model takes in input real-word facts from several sources, such as natural language text and knowledge bases, together with the context (e.g., the metadata of the newspaper article, the entity types, the words in the sentence) in which such facts have been extracted. We showed how to represent facts and relative contextual information employing an extended factorization machine model, that, differently from the original version, also works with positive only observations, under the open-world assumption. We discussed an efficient and parallel method for parameter estimation based on the Bayesian personalized ranking optimization criterion. Our experimental study on a real-world dataset validated the usefulness of contextual data in open relation extraction tasks; our CORE model provided higher prediction performance than state-of-the-art solutions.

We believe that the contributions presented have the potential of large practical applicability. The whole code used in the experiments has been released under the GPLv3 open source license and is available at `https://github.com/fabiopetroni`. Moreover, an implementation of our HDRF partitioning algorithm has been integrated inside GraphLab, a popular graph-based, high performance, distributed computation framework.

5.1 Future Work

We list some interesting directions for future research, dividing them in improvements that can be made to our methods and open research problems.

5.1.1 Improvements

We didn't investigate efficient implementations for our *HDRF* algorithm. Currently the algorithm, when processing an incoming edge, computes a score associated with each partition and selects the one with the largest value for it. We believe that some optimizations can be made to speed up the partitioning. For instance, the algorithm could check if the two vertices already share a partition before computing all scores, and maintain an incrementally updated balance factor in memory.

We conjecture that introducing a specific regularization term for each variables group in the CORE model, automatically updated during the learning procedure on a disjoint validation set, may increase the overall prediction quality. In fact, the CORE model is composed of several groups of variables, each with its peculiar predictive power. For instance, the group containing entity types might carry more information than the group containing articles metadata for the task of extracting new facts for a specific relation, and this should be reflected in the associated regularization terms.

5.1.2 Open research problems

An open research problem is how to distribute the training procedure for context-aware matrix completion algorithms. For instance, factorization machines are designed to work on a single core. We provided a lock-free solution to parallelize the training procedure among multiple processing cores working on shared memory. Exploring the feasibility of distributed solutions, able to work in a shared-nothing environment, is an interesting line of research. One possible approach could be an asynchronous restyling of the algorithm, where computing nodes work on a local copy of the data and synchronize periodically. In this case, however, the input data placement is very challenging, since the data can't be represented anymore as a graph but as an hypergraph. In fact, each training point (an hyperedge) connects several objects (vertices), e.g., relations, tuples, entities and several contextual information in the open relation extraction application scenario.

Another interesting investigation, connected with the previous point, is concerned with the adaptation of the *HDRF* graph partitioning algorithm to hypergraphs. The goal should always be (1) to minimize the vertex replication and (2) to balance the hyperedge load. We suppose that, also in this case, high degree vertices play a crucial role for the final quality of the partitioning.

A further line for future research might be the investigation of distributed solutions for the Bayesian personalized ranking optimization criterion. We remark that in a distributed shared-nothing environment each computing node has just a partial view on the entire input data. This setting is compliant, for instance, with the regularized square loss optimization criterion, where each update depend on a single training point included in the partial view. The Bayesian personalized ranking criterion, instead, requires the sampling of a negative counterpart for each given training point, that might not be present in the partial view of a computing node. A straightforward solution might, for instance, force the sampling procedure to draw only from the local portion of the dataset the current computing node owns. Some interesting questions in this regard are: does this affect the final quality of the algorithm? If yes, which countermeasures can be put in place?

Finally, scalable version of factorization machines and the BPR criterion might be composed to create a distributed matrix completion algorithm able to handle those cases in which only positive evidence exists in input.

Bibliography

[1] G. Adomavicius and A. Tuzhilin. Toward the next generation of recommender systems: A survey of the state-of-the-art and possible extensions. *IEEE Transactions on Knowledge and Data Engineering*, 17(6):734–749, 2005.

[2] G. Adomavicius and A. Tuzhilin. Context-aware recommender systems. In *Recommender systems handbook*, pages 217–253. Springer, 2011.

[3] A. Ahmed, N. Shervashidze, S. Narayanamurthy, V. Josifovski, and A. J. Smola. Distributed large-scale natural graph factorization. In *Proceedings of the 22nd international conference on World Wide Web*, 2013.

[4] A. Akbik, L. Visengeriyeva, P. Herger, H. Hemsen, and A. Löser. Unsupervised discovery of relations and discriminative extraction patterns. In *Proceedings of the 24th International Conference on Computational Linguistics (COLING)*, pages 17–32, 2012.

[5] R. Albert, H. Jeong, and A.-L. Barabási. Error and attack tolerance of complex networks. *Nature*, 406(6794):378–382, 2000.

[6] X. Amatriain. Recommender systems lecture, machine learning summer school (mlss) 2014. url: `https://youtu.be/bLhq63ygoU8`.

[7] K. Andreev and H. Räcke. Balanced graph partitioning. In *Proceedings of the 16th Annual ACM Symposium on Parallelism in Algorithms and Architectures*, 2004.

[8] S. Auer, C. Bizer, G. Kobilarov, J. Lehmann, R. Cyganiak, and Z. Ives. *Dbpedia: A nucleus for a web of open data*. Springer, 2007.

[9] S. Auer, J. Demter, M. Martin, and J. Lehmann. Lodstats–an extensible framework for high-performance dataset analytics. In *Knowledge Engineering and Knowledge Management*, pages 353–362. Springer, 2012.

[10] R. Baeza-Yates, B. Ribeiro-Neto, et al. *Modern information retrieval*, volume 463. ACM press New York, 1999.

[11] M. Banko, M. J. Cafarella, S. Soderl, M. Broadhead, and O. Etzioni. Open information extraction from the web. In *Proceedings of the 20th International Joint Conference on Artificial Intelligence (IJCAI)*, 2007.

[12] J. Bennett and S. Lanning. The netflix prize. In *Proceedings of KDD cup and workshop*, 2007.

[13] D. Billsus and M. J. Pazzani. Learning collaborative information filters. In *ICML*, volume 98, pages 46–54, 1998.

[14] D. M. Blei, A. Y. Ng, and M. I. Jordan. Latent dirichlet allocation. *the Journal of machine Learning research*, 3:993–1022, 2003.

[15] P. Boldi, M. Rosa, M. Santini, and S. Vigna. Layered label propagation: A multiresolution coordinate-free ordering for compressing social networks. In *Proceedings of the 20th international conference on World Wide Web*, 2011.

[16] P. Boldi and S. Vigna. The webgraph framework i: compression techniques. In *Proceedings of the 13th international conference on World Wide Web*, 2004.

[17] K. Bollacker, C. Evans, P. Paritosh, T. Sturge, and J. Taylor. Freebase: a collaboratively created graph database for structuring human knowledge. In *Proceedings of the 2008 ACM SIGMOD international conference on Management of data*, pages 1247–1250. ACM, 2008.

[18] O. Bousquet and L. Bottou. The tradeoffs of large scale learning. In *Advances in neural information processing systems*, pages 161–168, 2008.

[19] J. S. Breese, D. Heckerman, and C. Kadie. Empirical analysis of predictive algorithms for collaborative filtering. In *Proceedings of the Fourteenth conference on Uncertainty in artificial intelligence*, pages 43–52. Morgan Kaufmann Publishers Inc., 1998.

[20] D. S. Callaway, M. E. Newman, S. H. Strogatz, and D. J. Watts. Network robustness and fragility: Percolation on random graphs. *Physical review letters*, 85(25):5468, 2000.

[21] E. J. Candès and B. Recht. Exact matrix completion via convex optimization. *Foundations of Computational mathematics*, 9(6):717–772, 2009.

[22] K.-W. Chang, W.-t. Yih, B. Yang, and C. Meek. Typed tensor decomposition of knowledge bases for relation extraction. In *Proceedings of the 2014 Conference on Empirical Methods in Natural Language Processing (EMNLP)*, pages 1568–1579, 2014.

[23] K. Chen, T. Chen, G. Zheng, O. Jin, E. Yao, and Y. Yu. Collaborative personalized tweet recommendation. In *Proceedings of the 35th international ACM SIGIR conference on Research and development in information retrieval*, pages 661–670. ACM, 2012.

[24] A. L. Chistov and D. Y. Grigor'ev. Complexity of quantifier elimination in the theory of algebraically closed fields. In *Mathematical Foundations of Computer Science 1984*, pages 17–31. Springer, 1984.

[25] D. Cohen, D. Skillicorn, S. Gatehouse, and I. Dalrymple. Signature detection in geochemical data using singular value decomposition and semi-discrete decomposition. In *21st International Geochemical Exploration Symposium (IGES)*, 2003.

[26] R. Cohen, K. Erez, D. Ben-Avraham, and S. Havlin. Resilience of the internet to random breakdowns. *Physical review letters*, 85(21):4626, 2000.

[27] R. Cohen, K. Erez, D. Ben-Avraham, and S. Havlin. Breakdown of the internet under intentional attack. *Physical review letters*, 86(16):3682, 2001.

[28] R. Cyganiak and A. Jentzsch. The linking open data cloud diagram. url: `http://lod-cloud.net`.

[29] A. S. Das, M. Datar, A. Garg, and S. Rajaram. Google news personalization: scalable online collaborative filtering. In *Proceedings of the 16th international conference on World Wide Web*, pages 271–280. ACM, 2007.

[30] O. L. de Lacalle and M. Lapata. Unsupervised relation extraction with general domain knowledge. In *Proceedings of the 2013 Conference on Empirical Methods in Natural Language Processing (EMNLP)*, pages 415–425, 2013.

[31] J. Dean, G. Corrado, R. Monga, K. Chen, M. Devin, Q. V. Le, M. Z. Mao, M. Ranzato, A. W. Senior, P. A. Tucker, et al. Large scale distributed deep networks. In *Conference on Neural Information Processing Systems*, 2012.

[32] L. Del Corro and R. Gemulla. Clausie: clause-based open information extraction. In *Proceedings of the 22nd International Conference on World Wide Web (WWW)*, 2013.

[33] M. Deshpande and G. Karypis. Item-based top-n recommendation algorithms. *ACM Transactions on Information Systems (TOIS)*, 22(1):143–177, 2004.

[34] S. N. Dorogovtsev and J. F. Mendes. Evolution of networks. *Advances in physics*, 51(4):1079–1187, 2002.

[35] G. Dror, N. Koenigstein, Y. Koren, and M. Weimer. The yahoo! music dataset and kdd-cup'11. *Journal of Machine Learning Research-Proceedings Track*, 18:8–18, 2012.

[36] L. Drumond, S. Rendle, and L. Schmidt-Thieme. Predicting rdf triples in incomplete knowledge bases with tensor factorization. In *Proceedings of the 27th Annual ACM Symposium on Applied Computing (SAC)*, 2012.

[37] C. Eaton, D. Deroos, T. Deutsch, G. Lapis, and P. Zikopoulos. *Understanding Big Data.* Mc Graw Hill, 2012.

[38] T. Economist. The phone of the future. url: `http://www.economist.com/node/8312260`.

[39] M. D. Ekstrand, J. T. Riedl, and J. A. Konstan. Collaborative filtering recommender systems. *Foundations and Trends in Human-Computer Interaction*, 4(2):81–173, 2011.

[40] A. Fader, S. Soderland, and O. Etzioni. Identifying relations for open information extraction. In *Proceedings of the 2011 Conference on Empirical Methods in Natural Language Processing (EMNLP)*, 2011.

[41] M. Fan, D. Zhao, Q. Zhou, Z. Liu, T. F. Zheng, and E. Y. Chang. Distant supervision for relation extraction with matrix completion. In *Proceedings of the 52nd Annual Meeting of the Association for Computational Linguistics (ACL)*, 2014.

[42] U. Feige, M. Hajiaghayi, and J. R. Lee. Improved approximation algorithms for minimum weight vertex separators. *SIAM Journal on Computing*, 38(2):629–657, 2008.

[43] T. Franz, A. Schultz, S. Sizov, and S. Staab. Triplerank: Ranking semantic web data by tensor decomposition. In *Proceedings of the 8th International Semantic Web Conference (ISWC)*, 2009.

[44] S. Funk. Netflix update: Try this at home. url: `http://sifter.org/simon/Journal/20061211.html`.

[45] R. Gemulla, E. Nijkamp, P. J. Haas, and Y. Sismanis. Large-scale matrix factorization with distributed stochastic gradient descent. In *Proceedings of the 17th ACM SIGKDD international conference on Knowledge discovery and data mining*, 2011.

[46] D. Goldberg, D. Nichols, B. M. Oki, and D. Terry. Using collaborative filtering to weave an information tapestry. *Communications of the ACM*, 35(12):61–70, 1992.

[47] J. E. Gonzalez, Y. Low, H. Gu, D. Bickson, and C. Guestrin. Powergraph: Distributed graph-parallel computation on natural graphs. In *Proceedings of the 10th USENIX Symposium on Operating Systems Design and Implementation (OSDI)*, 2012.

[48] H. Halberstam and R. Laxton. Perfect difference sets. In *Proceedings of the Glasgow Mathematical Association*, 1964.

[49] A. Halevy, P. Norvig, and F. Pereira. The unreasonable effectiveness of data. *Intelligent Systems, IEEE*, 24(2):8–12, 2009.

[50] T. Hasegawa, S. Sekine, and R. Grishman. Discovering relations among named entities from large corpora. In *Proceedings of the 42nd Annual Meeting on Association for Computational Linguistics (ACL)*, 2004.

[51] J. L. Herlocker, J. A. Konstan, A. Borchers, and J. Riedl. An algorithmic framework for performing collaborative filtering. In *Proceedings of the 22nd annual international ACM SIGIR conference on Research and development in information retrieval*, pages 230–237. ACM, 1999.

[52] T. Hofmann. Latent semantic models for collaborative filtering. *ACM Transactions on Information Systems (TOIS)*, 22(1):89–115, 2004.

[53] Y. Huang, V. Tresp, M. Nickel, A. Rettinger, and H.-P. Kriegel. A scalable approach for statistical learning in semantic graphs. *Semantic Web*, 5(1):5–22, 2014.

[54] N. Jain, G. Liao, and T. L. Willke. Graphbuilder: Scalable graph etl framework. In *1st International Workshop on Graph Data Management Experiences and Systems*, 2013.

[55] X. Jiang, V. Tresp, Y. Huang, and M. Nickel. Link prediction in multi-relational graphs using additive models. In *Proceed-*

ings of the 2012 International Workshop on Semantic Technologies meet Recommender Systems & Big Data (SeRSy), 2012.

[56] X. Jin, Y. Zhou, and B. Mobasher. Web usage mining based on probabilistic latent semantic analysis. In *Proceedings of the tenth ACM SIGKDD international conference on Knowledge discovery and data mining*, pages 197–205. ACM, 2004.

[57] U. Kang, C. E. Tsourakakis, and C. Faloutsos. Pegasus: A peta-scale graph mining system implementation and observations. In *Data Mining, 2009. ICDM'09. Ninth IEEE International Conference on*, pages 229–238. IEEE, 2009.

[58] A. Karatzoglou, X. Amatriain, L. Baltrunas, and N. Oliver. Multiverse recommendation: n-dimensional tensor factorization for context-aware collaborative filtering. In *Proceedings of the fourth ACM conference on Recommender systems*, pages 79–86. ACM, 2010.

[59] G. Karypis and V. Kumar. A fast and high quality multilevel scheme for partitioning irregular graphs. *SIAM Journal on scientific Computing*, 20(1):359–392, 1998.

[60] M. Kim and K. S. Candan. SBV-Cut: Vertex-cut based graph partitioning using structural balance vertices. *Data & Knowledge Engineering*, 72:285–303, 2012.

[61] T. G. Kolda and B. W. Bader. Tensor decompositions and applications. *SIAM review*, 51(3):455–500, 2009.

[62] J. A. Konstan, B. N. Miller, D. Maltz, J. L. Herlocker, L. R. Gordon, and J. Riedl. Grouplens: applying collaborative filtering to usenet news. *Communications of the ACM*, 40(3):77–87, 1997.

[63] J. A. Konstan and J. Riedl. Recommender systems: from algorithms to user experience. *User Modeling and User-Adapted Interaction*, 22(1-2):101–123, 2012.

[64] Y. Koren. Factorization meets the neighborhood: a multifaceted collaborative filtering model. In *Proceedings of the 14th ACM SIGKDD international conference on Knowledge discovery and data mining*, pages 426–434. ACM, 2008.

[65] Y. Koren. Collaborative filtering with temporal dynamics. *Communications of the ACM*, 53(4):89–97, 2010.

[66] Y. Koren, R. Bell, and C. Volinsky. Matrix factorization techniques for recommender systems. *Computer*, 42(8):30–37, 2009.

[67] X. Li, G. Cong, X.-L. Li, T.-A. N. Pham, and S. Krishnaswamy. Rank-geofm: A ranking based geographical factorization method for point of interest recommendation. In *Proceedings of the 38th International ACM SIGIR Conference on Research and Development in Information Retrieval*, pages 433–442. ACM, 2015.

[68] G. Linden, B. Smith, and J. York. Amazon. com recommendations: Item-to-item collaborative filtering. *Internet Computing, IEEE*, 7(1):76–80, 2003.

[69] Y. Low, D. Bickson, J. Gonzalez, C. Guestrin, A. Kyrola, and J. M. Hellerstein. Distributed graphlab: a framework for machine learning and data mining in the cloud. *Proceedings of the VLDB Endowment*, 5(8):716–727, 2012.

[70] Y. Low, J. Gonzalez, A. Kyrola, D. Bickson, C. Guestrin, and J. M. Hellerstein. Graphlab: A new framework for parallel machine learning. In *Proceedings of the 26th Conference on Uncertainty in Artificial Intelligence*, 2010.

[71] H. Ma, H. Yang, M. R. Lyu, and I. King. Sorec: social recommendation using probabilistic matrix factorization. In *Proceedings of the 17th ACM conference on Information and knowledge management*, pages 931–940. ACM, 2008.

[72] H. Ma, T. C. Zhou, M. R. Lyu, and I. King. Improving recommender systems by incorporating social contextual information. *ACM Transactions on Information Systems (TOIS)*, 29(2):9, 2011.

[73] F. Makari, C. Teflioudi, R. Gemulla, P. Haas, and Y. Sismanis. Shared-memory and shared-nothing stochastic gradient descent algorithms for matrix completion. *Knowledge and Information Systems*, 42(3):493–523, 2014.

[74] G. Malewicz, M. H. Austern, A. J. Bik, J. C. Dehnert, I. Horn, N. Leiser, and G. Czajkowski. Pregel: a system for large-scale graph processing. In *Proceedings of the 2010 ACM SIGMOD International Conference on Management of data*, 2010.

[75] J. Mangalindan. Amazon's recommendation secret. `http://tech.fortune.cnn.com/2012/07/30/amazon-5` CNN Money, 2012.

[76] R. McDonald, K. Hall, and G. Mann. Distributed training strategies for the structured perceptron. In *Human Language Technologies: The 2010 Annual Conference of the North American Chapter of the Association for Computational Linguistics*, pages 456–464. Association for Computational Linguistics, 2010.

[77] A. K. Menon and C. Elkan. Link prediction via matrix factorization. In *Machine Learning and Knowledge Discovery in Databases*, pages 437–452. Springer, 2011.

[78] B. Min, R. Grishman, L. Wan, C. Wang, and D. Gondek. Distant supervision for relation extraction with an incomplete knowledge base. In *Proceedings of the 2013 Conference of the North American Chapter of the Association for Computational Linguistics: Human Language Technologies (HLT-NAACL)*, 2013.

[79] B. Min, S. Shi, R. Grishman, and C.-Y. Lin. Ensemble semantics for large-scale unsupervised relation extraction. In *Proceedings of the 2012 Joint Conference on Empirical Methods in Natural Language Processing and Computational Natural Language Learning (EMNLP-CoNLL)*, 2012.

[80] M. Mintz, S. Bills, R. Snow, and D. Jurafsky. Distant supervision for relation extraction without labeled data. In *Proceedings of the Joint conference of the 47th Annual Meeting*

of the Association for Computational Linguistics and the 4th International Joint Conference on Natural Language Processing of the Asian Federation of Natural Language Processing (ACL-IJCNLP), 2009.

[81] A. Mnih and R. Salakhutdinov. Probabilistic matrix factorization. In *Advances in neural information processing systems*, pages 1257–1264, 2007.

[82] S. Moghaddam, M. Jamali, and M. Ester. Etf: extended tensor factorization model for personalizing prediction of review helpfulness. In *Proceedings of the fifth ACM international conference on Web search and data mining*, pages 163–172. ACM, 2012.

[83] A. Nedić and D. Bertsekas. Convergence rate of incremental subgradient algorithms. In *Stochastic optimization: algorithms and applications*, pages 223–264. Springer, 2001.

[84] A. H. B. News). The age of information overload. url: `http://news.bbc.co.uk/2/hi/programmes/click_online/9742180.stm`.

[85] M. Nickel, V. Tresp, and H.-P. Kriegel. A three-way model for collective learning on multi-relational data. In *Proceedings of the 28th international conference on machine learning (ICML)*, 2011.

[86] M. Nickel, V. Tresp, and H.-P. Kriegel. Factorizing yago: scalable machine learning for linked data. In *Proceedings of the*

21st International Conference on World Wide Web (WWW), 2012.

[87] F. Niu, B. Recht, C. Ré, and S. J. Wright. Hogwild!: A lock-free approach to parallelizing stochastic gradient descent. *Advances in Neural Information Processing Systems*, 24:693–701, 2011.

[88] Y. Niu, Y. Wang, G. Sun, A. Yue, B. Dalessandro, C. Perlich, and B. Hamner. The tencent dataset and kdd-cup'12. In *KDD-Cup Workshop*, volume 170, 2012.

[89] W. Pan, H. Zhong, C. Xu, and Z. Ming. Adaptive bayesian personalized ranking for heterogeneous implicit feedbacks. *Knowledge-Based Systems*, 73:173–180, 2015.

[90] F. Petroni, L. D. Corro, and R. Gemulla. Core: Context-aware open relation extraction with factorization machines. In *Proceedings of the 2015 Conference on Empirical Methods in Natural Language Processing (EMNLP)*, 2015.

[91] F. Petroni and L. Querzoni. Gasgd: stochastic gradient descent for distributed asynchronous matrix completion via graph partitioning. In *Proceedings of the 8th ACM Conference on Recommender Systems (RecSys)*, pages 241–248. ACM, 2014.

[92] F. Petroni, L. Querzoni, K. Daudjee, S. Kamali, and G. Iacoboni. Hdrf: Stream-based partitioning for power-law graphs. In *Proceedings of the 24th ACM International Conference on Conference on Information and Knowledge Management (CIKM)*, 2015.

[93] Y. C. R. Chen, J. Shi and H. Chen. Powerlyra: Differentiated graph computation and partitioning on skewed graphs. In *Proceedings of the 10th ACM SIGOPS European Conference on Computer Systems*, 2015.

[94] B. Recht and C. Ré. Parallel stochastic gradient algorithms for large-scale matrix completion. *Mathematical Programming Computation*, 5(2):201–226, 2013.

[95] B. Recht, C. Re, S. Wright, and F. Niu. Hogwild: A lock-free approach to parallelizing stochastic gradient descent. In *Proceedings of the 25th Annual Conference on Neural Information Processing Systems (NIPS)*, 2011.

[96] S. Rendle. *Context-aware ranking with factorization models.* Springer, 2011.

[97] S. Rendle. Factorization machines with libfm. *ACM Transactions on Intelligent Systems and Technology (TIST)*, 3(3):57, 2012.

[98] S. Rendle. Scaling factorization machines to relational data. In *Proceedings of the VLDB Endowment*, volume 6, pages 337–348. VLDB Endowment, 2013.

[99] S. Rendle, C. Freudenthaler, Z. Gantner, and L. Schmidt-Thieme. Bpr: Bayesian personalized ranking from implicit feedback. In *Proceedings of the 25th Conference on Uncertainty in Artificial Intelligence (UAI)*, 2009.

[100] S. Rendle, Z. Gantner, C. Freudenthaler, and L. Schmidt-Thieme. Fast context-aware recommendations with factoriza-

tion machines. In *Proceedings of the 34th international ACM conference on Research and development in Information Retrieval (SIGIR)*, 2011.

[101] S. Rendle and L. Schmidt-Thieme. Pairwise interaction tensor factorization for personalized tag recommendation. In *Proceedings of the third ACM international conference on Web search and data mining*, pages 81–90. ACM, 2010.

[102] P. Resnick, N. Iacovou, M. Suchak, P. Bergstrom, and J. Riedl. Grouplens: an open architecture for collaborative filtering of netnews. In *Proceedings of the 1994 ACM conference on Computer supported cooperative work*, pages 175–186. ACM, 1994.

[103] F. Ricci, L. Rokach, and B. Shapira. *Introduction to recommender systems handbook*. Springer, 2011.

[104] S. Riedel, L. Yao, A. McCallum, and B. M. Marlin. Relation extraction with matrix factorization and universal schemas. In *Proceedings of the 2013 Conference of the North American Chapter of the Association for Computational Linguistics: Human Language Technologies (HLT-NAACL)*, 2013.

[105] R. Salakhutdinov, A. Mnih, and G. Hinton. Restricted boltzmann machines for collaborative filtering. In *Proceedings of the 24th international conference on Machine learning*, pages 791–798. ACM, 2007.

[106] M. Saleem. Collaborative filtering: Lifeblood of the social web. url: `http://readwrite.com/2008/06/30/collaborative_filtering_social_web`.

[107] E. Sandhaus. The New York Times Annotated Corpus. *Linguistic Data Consortium, Philadelphia*, 6(12), 2008.

[108] B. Sarwar, G. Karypis, J. Konstan, and J. Riedl. Application of dimensionality reduction in recommender system-a case study. Technical report, DTIC Document, 2000.

[109] B. Sarwar, G. Karypis, J. Konstan, and J. Riedl. Item-based collaborative filtering recommendation algorithms. In *Proceedings of the 10th international conference on World Wide Web*, pages 285–295. ACM, 2001.

[110] B. Schwartz. The paradox of choice: Why more is less. Ecco New York, 2004.

[111] G. Shani, R. I. Brafman, and D. Heckerman. An mdp-based recommender system. In *Proceedings of the Eighteenth conference on Uncertainty in artificial intelligence*, pages 453–460. Morgan Kaufmann Publishers Inc., 2002.

[112] Y. Shi, A. Karatzoglou, L. Baltrunas, M. Larson, A. Hanjalic, and N. Oliver. Tfmap: Optimizing map for top-n context-aware recommendation. In *Proceedings of the 35th international ACM SIGIR conference on Research and development in information retrieval*, pages 155–164. ACM, 2012.

[113] Y. Shi, M. Larson, and A. Hanjalic. Exploiting user similarity based on rated-item pools for improved user-based collaborative filtering. In *Proceedings of the third ACM conference on Recommender systems*, pages 125–132. ACM, 2009.

[114] Y. Shi, M. Larson, and A. Hanjalic. Collaborative filtering beyond the user-item matrix: A survey of the state of the art and future challenges. *ACM Computing Surveys (CSUR)*, 47(1):3, 2014.

[115] Y. Shinyama and S. Sekine. Preemptive information extraction using unrestricted relation discovery. In *Proceedings of the 2006 Conference of the North American Chapter of the Association for Computational Linguistics: Human Language Technologies (HLT-NAACL)*, 2006.

[116] A. P. Singh and G. J. Gordon. Relational learning via collective matrix factorization. In *Proceedings of the 14th ACM SIGKDD international conference on Knowledge discovery and data mining*, pages 650–658. ACM, 2008.

[117] A. Singhal. Introducing the knowledge graph: things, not strings. url: `http://googleblog.blogspot.co.uk/2012/05/introducing-knowledge-graph-things-not.html`.

[118] A. Singhal. Modern information retrieval: A brief overview. *IEEE Data Eng. Bull.*, 24(4):35–43, 2001.

[119] D. Skillicorn. *Understanding complex datasets: data mining with matrix decompositions*. CRC press, 2007.

[120] C. Smith. By the numbers: 80+ amazing amazon statistics. url: `http://expandedramblings.com/index.php/amazon-statistics`.

[121] X. Su and T. M. Khoshgoftaar. A survey of collaborative filtering techniques. *Advances in Artificial Intelligence*, 2009:4, 2009.

[122] M. Surdeanu, J. Tibshirani, R. Nallapati, and C. D. Manning. Multi-instance multi-label learning for relation extraction. In *Proceedings of the 2012 Joint Conference on Empirical Methods in Natural Language Processing and Computational Natural Language Learning (EMNLP-CoNLL)*, 2012.

[123] G. Takács, I. Pilászy, B. Németh, and D. Tikk. Scalable collaborative filtering approaches for large recommender systems. *The Journal of Machine Learning Research*, 10:623–656, 2009.

[124] S. Takamatsu, I. Sato, and H. Nakagawa. Probabilistic matrix factorization leveraging contexts for unsupervised relation extraction. In *Advances in Knowledge Discovery and Data Mining*, pages 87–99. Springer, 2011.

[125] C. Teflioudi, F. Makari, and R. Gemulla. Distributed matrix completion. In *International Conference on Data Mining*, 2012.

[126] V. Tresp, Y. Huang, M. Bundschus, and A. Rettinger. Materializing and querying learned knowledge. In *Proceedings of the 2009 International Workshop on Inductive Reasoning and Machine Learning for the Semantic Web (IRMLeS)*, 2009.

[127] J. N. Tsitsiklis, D. P. Bertsekas, M. Athans, et al. Distributed asynchronous deterministic and stochastic gradient

optimization algorithms. *IEEE transactions on automatic control*, 31(9):803–812, 1986.

[128] C. Tsourakakis, C. Gkantsidis, B. Radunovic, and M. Vojnovic. Fennel: Streaming graph partitioning for massive scale graphs. In *Proceedings of the 7th ACM international conference on Web search and data mining*, 2014.

[129] F. Viger and M. Latapy. Efficient and simple generation of random simple connected graphs with prescribed degree sequence. In *Computing and Combinatorics*. Springer, 2005.

[130] R. West, E. Gabrilovich, K. Murphy, S. Sun, R. Gupta, and D. Lin. Knowledge base completion via search-based question answering. In *Proceedings of the 23rd international conference on World wide web*, pages 515–526. ACM, 2014.

[131] C. Xie, L. Yan, W.-J. Li, and Z. Zhang. Distributed power-law graph computing: Theoretical and empirical analysis. In *Advances in Neural Information Processing Systems*, 2014.

[132] L. Yao, A. Haghighi, S. Riedel, and A. McCallum. Structured relation discovery using generative models. In *Proceedings of the 2011 Conference on Empirical Methods in Natural Language Processing (EMNLP)*, pages 1456–1466, 2011.

[133] J. Zhang and P. Pu. A recursive prediction algorithm for collaborative filtering recommender systems. In *Proceedings of the 2007 ACM conference on Recommender systems*, pages 57–64. ACM, 2007.

[134] Y. Zhen, W.-J. Li, and D.-Y. Yeung. Tagicofi: tag informed collaborative filtering. In *Proceedings of the third ACM conference on Recommender systems*, pages 69–76. ACM, 2009.

[135] V. W. Zheng, Y. Zheng, X. Xie, and Q. Yang. Collaborative location and activity recommendations with gps history data. In *Proceedings of the 19th international conference on World wide web*, pages 1029–1038. ACM, 2010.

[136] Y. Zhuang, W.-S. Chin, Y.-C. Juan, and C.-J. Lin. A fast parallel sgd for matrix factorization in shared memory systems. In *Proceedings of the 7th ACM conference on Recommender systems*, 2013.

[137] P. Zigoris and Y. Zhang. Bayesian adaptive user profiling with explicit &amp; implicit feedback. In *Proceedings of the 15th ACM international conference on Information and knowledge management*, pages 397–404. ACM, 2006.